UNIVERSITY OF SUNDERLAND

Final Year Project

Model Electric Car based on Tesla S P85 & Design Speed Control System

AWAB SYED

5/2/2019

Name: Awabullah M. Syed

Student Number: 118 616 4302

University Name: University of Sunderland

Course: BEng Mechanical Engineering

Supervisor: Kevin Burn & Peter Usher

Submission Date: 2nd May 2019

Awab Syed

Declaration

I hereby declare:

that all the work presented in the report is of my own except otherwise referenced;

that this report is not been previously acknowledged nor submitted before as part of the final year dissertation;

that I have not deliberately allowed any student or anyone to replicate the report.

I understand and ensure that the work of others that are used in this report to form the basis of the report are well referenced. I also ensure the quality and the integrity of the report and affirm that I understand the University regulations to my full understanding. I confirm that the report is independent and impartial with no discrimination towards anyone or towards any specific method.

Signed: Awabullah Syed

Date: 24th April 24, 2019

Abstract

The objective of the project was to model electric car based on Tesla S P85 and to design a speed control system implementing various algorithms to tune the controllers. The report reviewed existing pieces of literature, articles, journals, books and published academic work to gather relevant data to represent the Tesla S P85 mathematically. The mathematical model consisting of vehicle dynamics, battery, motor, aerodynamic drag and other germane components were examined and scrutinised from an engineering perspective. Transfer functions and MATLAB functional blocks were then used to transform the mathematical form into MATLAB Simulink model replicating the real-world Tesla S P85 and the speed control system. Suitable limitations particularly restricting the performance of the battery were applied to ensure that the Simulink imitates the Tesla model. Moreover, assumptions were made throughout the design and build phase of the model to ensure that the report is kept well within the scope.

Various controllers; P, PI, PID were implemented in the control system and were manually finely tuned inspired by Zeigler-Nichols method as well as through the use of Auto-tune MATLAB function. The results obtained from the Simulink model were evaluated and compared against the specified performance criteria of the speed control system.

P-controller implemented in the speed control system and tuned through the Zeigler-Nichols method was unable to reach the desired/reference input speed and had a constant steady-state error. In order for the system to reach the reference input speed, a manually tuned PI-controller was implemented by introducing I-integral gain. Though, the difference between the reference input speed and the output came very close (1.8%) however, failed to reach the exact value. Hence, a constant steady-state error of 1.8% existed. Therefore, a PID-controller was introduced by the addition of D-derivative gain. The PID controller was tuned using two different methods; manually, and MATLAB auto-tune. The PID controller tuned through MATLAB auto tune also had a steady-state error of 1.8% due to the amendment in the ‘Filter Coefficient’ (N) by the MATLAB, the effects of it were not considered nor analysed in this report. However, the manually tuned PID controller had no steady-state error and met all the other set performance criteria. Therefore, after in-depth comparison, it was concluded that the manually tuned inspired by Zeigler-Nichols method PID controller implemented in the speed control system replicating Tesla S P85 had the best performance in respect to the set performance criteria.

Acknowledgement

Throughout the project, the strong support and the believe provided by the family and friends helped to complete the project successfully.

The motivation, inspiration and critical advice/feedback given by the supervisor, Kevin Burn, helped to fight through the difficult and demanding time to deliver to the expectation. Hence, I would like to thank, Kevin Burn for sharing his knowledge and experience which provided the fundamental background required to initiate this report.

Last but not least, would like to dedicate this report to the deceased Professor, Alan Wheatley, who worked exceptionally hard to thoroughly educate students including me in areas of knowledge in which he was remarkable at.

Any miscalculation or inaccuracy within the report is entirely my own responsibility.

List of Acronyms/Nomenclature

A	Frontal Area (m^2)
AC	Alternating Current
AWD	All-wheel Drive
b	Damping Coefficient
C_D	Drag Coefficient
C_W	Wheel Circumference
C_r	Rolling Resistance Coefficient
D_F	Drag Force
DC	Direct Current
EV	Electric Vehicles
F	Force
F_R	Rolling Resistance
F_f	Resultant Force
g	Gravity
H	Henry (Inductance Unit)
HP	Horsepower
I	Current
J_M	Moment of inertia of the rotor kg.m^2
$K_1 = \frac{K_p}{T_1}$	Integral Gain
$K_D = K_p \times T_D$	Derivative Gain
K_E	Back EMF constant
K_P	Proportional Gain
K_T	Torque Constant
K_d	Derivative Gain
K_i	Integral Gain
L	Inductance
L_R	Distance from the center of the rotation
Nm	Newton meter
R	Actual Armature Resistance
r	Reference Variable

R_e	Electric Resistance
R_T	Total Resistance (N)
R_g	Gear Ratio
R_r	Actual Rolling Resistance (Constant)
RPM	Revolutions per minute
RWD	Rear-wheel drive
S	Complex Number
s	Seconds
Specs	Specification
T	Temperature
T_1	Integral Time Constant
T_d	Derivative Time Constant
T_i	Constant Integral Time
u	control signal
V	Velocity of Vehicle (m/s)
V	Voltage
ρ	Air Density (kg/m^3)
τ / T	Torque
Ω	Ohms (Resistance Unit)
ω	Rotational Velocity
$e(t)$	Error
μ	Coefficient of Friction

List of Figures

Contents

Project Management / Plan

Gantt Chart

Modelling Tesla S P85 & Designing Speed Control System - Gantt Chart

Week 1= 5th November 2018

Period Highlig 21

Plan Duration | Actual Start | % Complete | Actual (beyond plan) | % Complete (beyond plan)

ACTIVITY	PLAN START	PLAN DURATION	ACTUAL START	ACTUAL DURATION	PERCENT COMPLETE
Column1	Column	Column	Column	Column	Column6
Design Brief	1	2	1	2	100%
Research Topics	3	1	3	2	100%
Set out Objectives	3	1	3	1	100%
Articles / Secondary Rsh	4	3	3	4	100%
Build Simple MATLAB models	8	2	7	3	100%
Create Simulink Model	10	1	10	1	100%
Document Literature Review	11	5	11	7	100%
Build mathematical	16	2	16	2	100%
complete Simulink Model	16	2	15	3	100%
Consider relevant controllers	18	1	18	1	100%
Consider relevant tuning methods	19	1	19	1	100%
Open and closed loop response	20	1	18	2	100%
Implement the control system	21	1	20	2	100%
Tuning, Analzing and Documentation,	21	6	21	4	100%

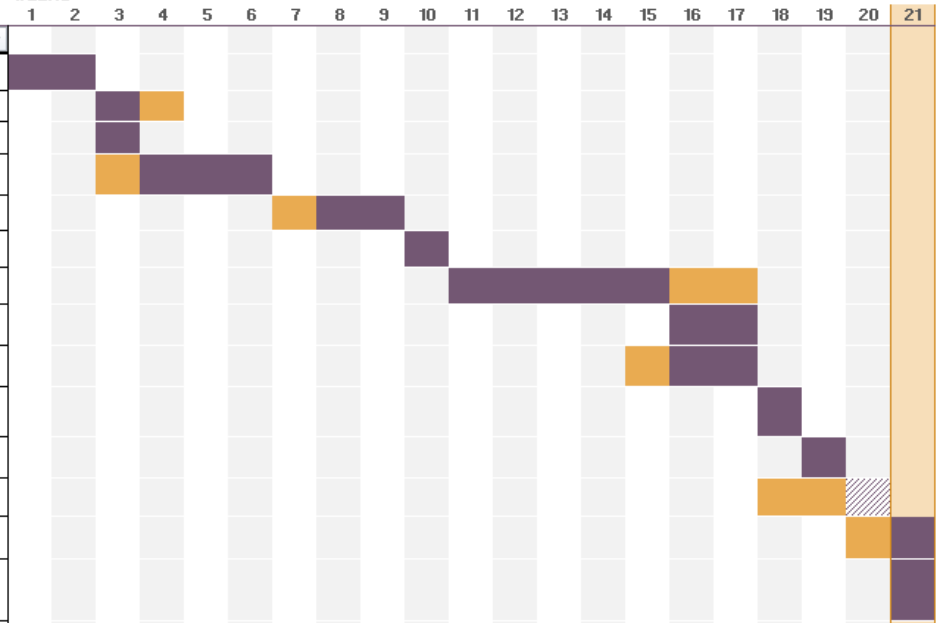

Network Diagram

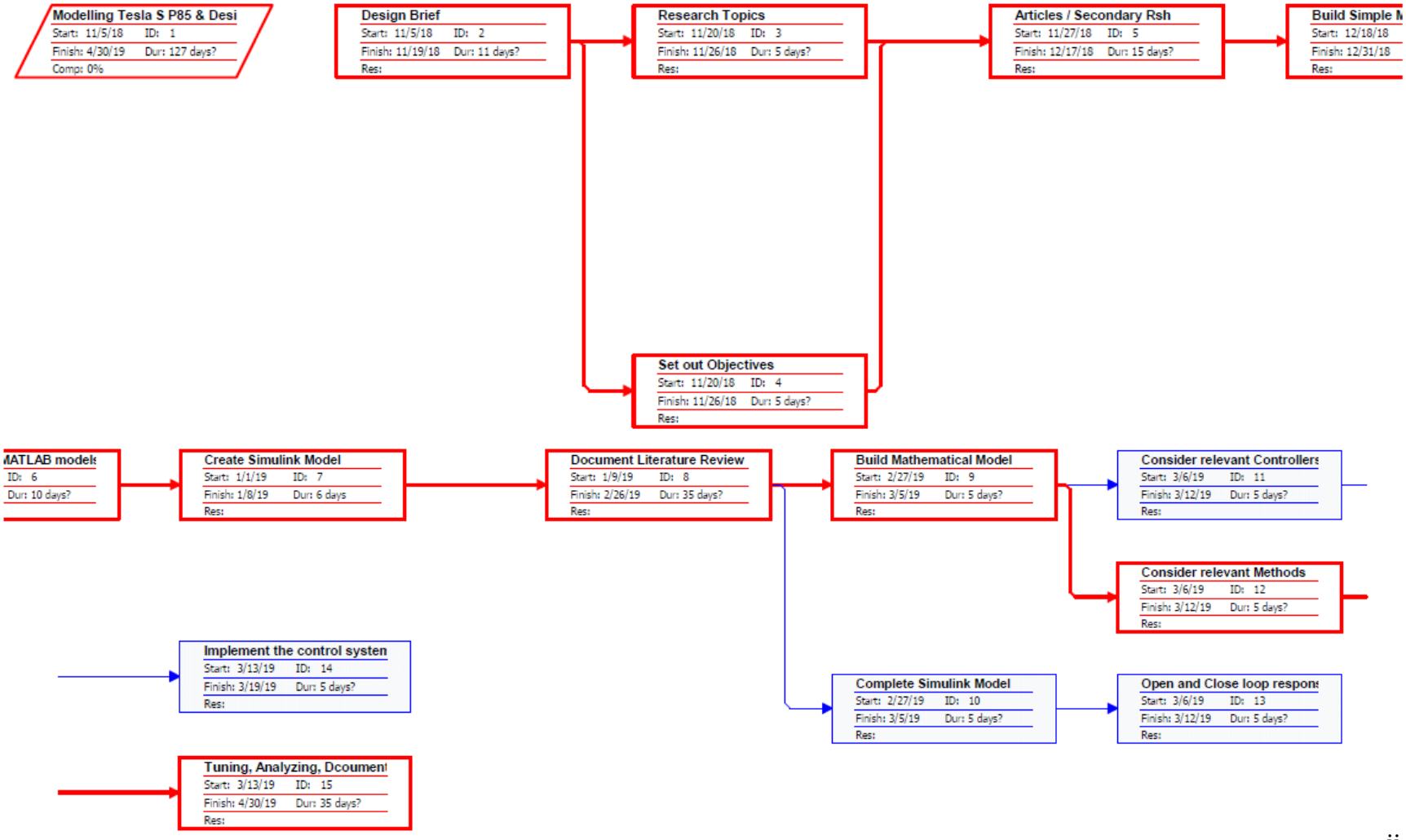

The Gantt chart and the network diagram both exhibits the project management plan used/followed throughout the project journey, allowing to keep track of work and meet deadlines as well as to mitigate delays.

As apparent in the Gantt chart, *'Literature Review'* took two additional weeks to document than expected due to other unexpected workloads. However, the secondary research was done on time enabling the construction of the '*Mathematical Model'* to run side by side with the '*Literature Review'*. Thus, ensuring that the extension of '*Literature Review'* had minimal impact on the progress/deadlines. The amalgamation of implementing '*Controllers.'* with *'Closed loop response.'* allowed to further compensate for the delay in the documentation of '*Literature Review.'* by freeing up a week while the rest of the project came along fine, as planned. Furthermore, the need for a three-week cushion was recognised/added during the planning stage to mitigate delays caused by unforeseen workload, enabling to avoid any unexpected outcome.

Appendix B shows the summary of the notes/comments taken down during meetings with the supervisor.

1. Introduction

1.1. Summary

The motivation and inspiration to undertake a project related to control systems and the electric car came from the recent development of autonomous vehicles particularly 'Waymo', a Google-owned company and the global push to move towards electric vehicles (Gershgorn, 2018).

This project thoroughly analysed and assessed the Tesla Model S P85 to construct a mathematical model which was transformed into MATLAB Simulink. Moreover, implementing finely tuned controllers into the speed control system replicating Tesla S P85. The outcome of the project would determine the tuning method/algorithms and the controller that best suits the parameters of the speed control system.

It should be noted that necessary assumptions were made and pointed out throughout the project. The assumptions were made in such a manner to make the model simpler while meeting the set objectives.

One of the significant benefits expected from this project is to be able to gain a full understanding of electric vehicles and its dynamics while also being able to obtain in-depth knowledge of different types of control systems with their limitations.

1.2. Aims & Objectives

The goal was to model an electric vehicle replicating Tesla S P85 on MATLAB Simulink and design a control system to regulate the speed.

The objectives of the project are as follows:

- Examine the vehicle dynamics of Tesla Model S P85 from an engineering perspective, analyse and scrutinise relevant components, i.e. the battery, wheels and motor of the vehicle.
- Derive and develop the mathematical model behind the vehicle dynamics.
- Determine the forces acting on the vehicle as it moves
- Implement an engineering model in MATLAB SIMULINK using main functional blocks, transfer functions.
- Identify and evaluate relevant techniques to design control systems to regulate the speed of the Tesla Model S P85.
- Implement, test and tune the controllers of the speed control system that correlates to the specified requirements/parameters.

- Compare the performance of each modelled speed control systems.

1.3. Scope

The project will begin with a review of existing literature, involving patent search, articles, and books and published academic work etc. (Knowles, 2016-17). A mathematical model representing the Tesla Model S P85 will be constructed to execute an in-depth analysis of the vehicle's dynamics to evaluate the battery performance, motor, wheels and other potential components that could influence the Simulink model. The mathematical model would then be translated to the MATLAB Simulink with the help of functional blocks, transfer functions and closed-loop model.

Control systems are to be designed using MATLAB to regulate the speed of the electric car; Tesla Model S P85. A range of controllers would be considered and compared with respect to their limitations. The controllers implemented in the control system would be tuned using algorithms to suit the set parameters.

1.4. Background / Industrial Context

The concept of electric cars could be traced back to 1828, Hungarian inventor, Anyos Jedlik constructed a prototype to power a small model carriage (Moss, 2018). However, the conception of vehicles powered by electric slowly begins to deteriorate and reached a 'dead period' during the 1930s due to the rise in the petroleum industry. The re-birth of interest in electric cars began in the 1960s, led by Renault while the 'Electric Vehicle Act of 1976' immensely boosted publics' interest (Wakefield, 1993). The environmental impact also played an important factor in enhancing and paving the pathway for electric cars as an alternative for petroleum-based vehicles.

Tesla, Inc founded in 2003, released the first vehicle; Roadster in 2008; however, the performance of Tesla S P85 revolutionised the electric cars industry in 2013. A 2013 Tesla Model S P85 was analysed and evaluated since it is the most popular amongst other models with respect to the number of vehicles sold (Erik Gregersen, 2018).

The electric vehicle and the speed control system, both have the potential to become a leading and global industry as the driverless vehicle are expected to hit the market in 2019, in conjunction with an expected significant increase in the sales of the electric car. The expected release of WAYMO; Google-owned driverless electric car would also affect the electric vehicles' market.

In the modern era, every car, be it electric, petrol, internal combustion or any other gas fed engines as the driving force, all contain control systems to an extent. The fuel injection system was the first revolutionary step towards making the automobile industry automated and regulating the speed of the vehicle (Kirkland, 2017). As the industry adopted the speed control system and headed towards autopilot driverless vehicles, it progressively embraced the electrification, lately led by Tesla. It was estimated that “By 2040, 54 percent of all cars sold on the planet will be electric” (Hawkins, How Tesla changed the auto industry forever, 2017). Hence, the outcome of this project is of great value as it identifies speed control systems of electric cars. It is the aim of this project to model Tesla S P85 and design speed control system via MATLAB Simulink.

2. Literature Review

2.1. Electric Vehicle Act & Petroleum Comparison

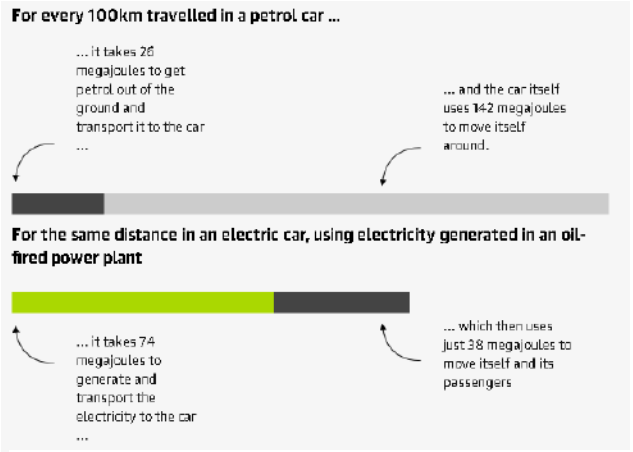

Figure 1 - General comparison between petrol and electrically driven cars (Clarke, 2017)

'Electric Vehicle Act of 1976' was vetoed by the US government that promoted the electric vehicles in order to 'reduce the dependence on oil'. This Act provided $160 million to be spent on the research and development (R&D) of electric and hybrid vehicles while also to carry out a feasibility study to show commercial feasibility of electric vehicles (Government, 1976).

Figure 1 shows a universal comparison between petroleum based and electrically driven vehicles. It was evident that electric powered cars use only two third of the energy of a petrol car to travel the same distance. Hence, deduced that electric cars would be in the majority in the near future considering the political influence. Tesla Model S; the current finest electrically powered vehicle was selected as a prototype to design a speed control system (Hawkins, How Tesla changed the auto industry forever, 2017). It should be noted that the environmental impact was not analysed in-depth as it was out of the scope of this report.

2.2. Tesla Model S P85

2013 Tesla Model S P85 revolutionised the electric car industry due to its cutting ledge battery performance and battling acceleration, reaching 100 km/h within 4.4 seconds (Tesla - Model S - P85 PERFORMANCE (416Hp)). The acceleration of the model was vital while tuning the Simulink Model to ensure that it replicated the practical/real Tesla Model S P85. Other characteristics and features especially the weight of the car was also necessary and extracted from (Cain, 2014). Though the newer version of the Tesla Model S series has much better performance index but due to the steer in the industry made by the initial release, it was best to analyse the preliminary one (S P85).

According to ISO 3833 standards (International Organization for Standardization, 1977), Tesla Model S P85 falls in the category of 'electrically powered family Sedan'. The characteristics, dimensions and the shape of the vehicle played a vital role in the modelling process since it

dictated the aerodynamic resistance. Aerodynamics resistance affected the acceleration of the vehicle while also impacted the efficiency of the battery. One of the ways to tackle this could potentially be to tune the model in accordance with the real acceleration. As discussed before, setting a bar of reaching 100 km/h in 4.4 seconds could be the initial step towards making the Simulink model behave in a similar manner to the actual vehicle.

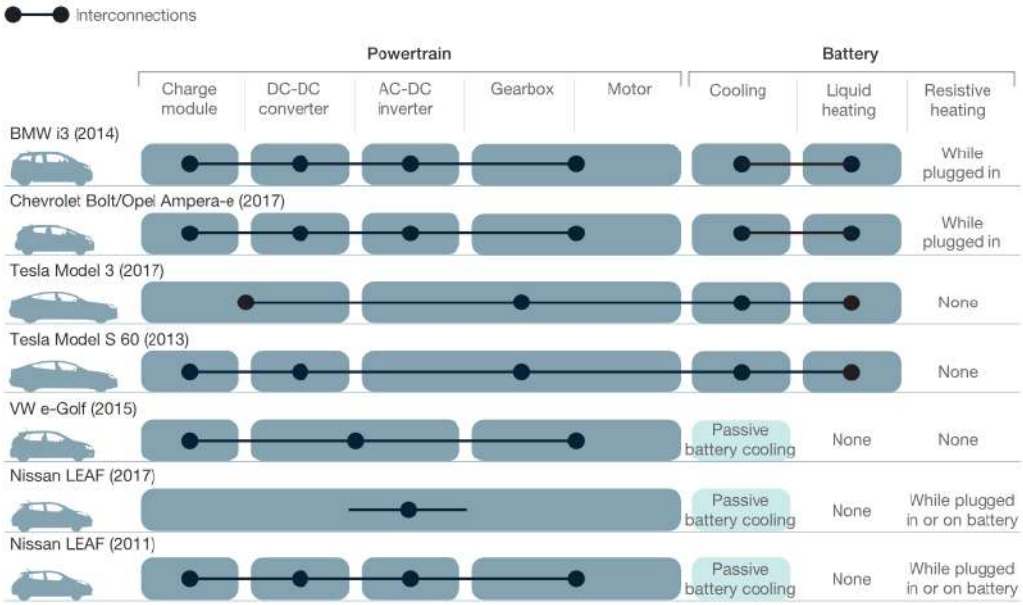

Figure 2 - Electric-vehicle powertrain thermal management system (Mckinsey Center for Future Mobility, 2018)

Figure 2 exhibits and compares the powertrain and the thermal management system of various popular electric vehicles. The article written by (Mckinsey Center for Future Mobility, 2018) clearly showed that there was a significant move towards more 'simple and efficient thermal management'. This article was of good use as it helped to analyse the limitations of the battery though, the article did not indulge from the mathematical perspective which would have been useful to model the vehicle mathematically.

2.3. Ethics / Corporate Social Responsibility (CSR) & Environmental, Social, Governance (ESG) Metric

Tesla, a company, widely reputed for being very environmental-conscious electric automaker (Dudovskiy, 2018) however, it had never engaged in corporate social / sustainability reporting and ESG matric until recently announced that a detailed report to be published that would cover all aspect, due to growing pressure from various stakeholders.

Figure 3 shows a CSR / ESG ranking of 21%, thanks to its low carbon emission. A ranking that sits well within the low range spectrum was primarily due to its negligence on climate change issues. The director of ethics and engagement for the Church of England Pension Board and co-chair of TPI (Transition Pathway Initiative) said "They are by far the most efficient in terms of alignment with 2°, but at the same time they're one of the worst in terms of actually making public disclosure of climate change management as a business" (mcMahon, 2018).

Figure 3 - CSR / ESG Ranking of Tesla (CSRHUB Team , n.d.)

Figure 4 shows the ratings given by (CSRHUB Team , n.d.) to the Tesla Inc, exemplifying their policies and ethics in different sects of the business. It was very apparent that Tesla had a very similar (singular) approach throughout different business sectors.

Figure 4 - 12 subcategories of Ratings and Rakings (CSRHUB Team , n.d.)

To prevent accidents and hefty collisions, an 'Automatic Emergency Braking' system was installed which instantaneously halts the car when an object is sensed in front. This would override the speed control system however, AEB would be deactivated when the system receives signals from the accelerator. Although, there were some disagreements amongst the expert that human judgement cannot be a privileged (Lin, 2017).

Figure 5 - Tesla's Autopilot steered car toward barrier (Hawkins, Tesla's Autopilot steered car toward barrier before deadly crash, investigators say, 2018)

Figure 5 shows the Tesla Model X after the fatal crash that caused the driver's life. The vehicle was on cruise control with the autopilot mode on and autosteered into a barrier. The AEB did not respond as the driver had his hand on the steering. Therefore, ethics and whether human judgement should be relied upon is a significant area that could potentially affect the company's image. However, ethics, CSG and ESG metrics are not discussed nor analysed in-depth throughout the report as it is out of the scope.

A popular email revealed the aggressive legal and media approach of Tesla which stated: "If there is media attention, there will be no deal" (Levin, 2018). This certainly showed that firstly, the company takes its public image seriously and secondly, was willing to go to any extent to avoid negative publicity; however, this could backfire which it did in this case.

2.4. Tesla S P85 Vehicle Dynamics

2.4.1. Input

Pedals of the car represented the input which produces the desired speed. A speed controller was placed to act as pedals in the MATLAB model to produce specific velocity. The input was significantly affected by battery performance and reviewed in the section below.

Figure 6 shows the correlation between the external forces and the speed of the vehicle. Aerodynamic drag increased with the vehicle speed as concluded by (Taherian, 2014) while the rolling resistance between the tyres and the road remained constant. Although the relationship between the aerodynamics and the vehicle speed would be the same when considering the Tesla model, however, the values would be different due to numerous factors including the boundary conditions and the streamline of the Tesla model's body surface.

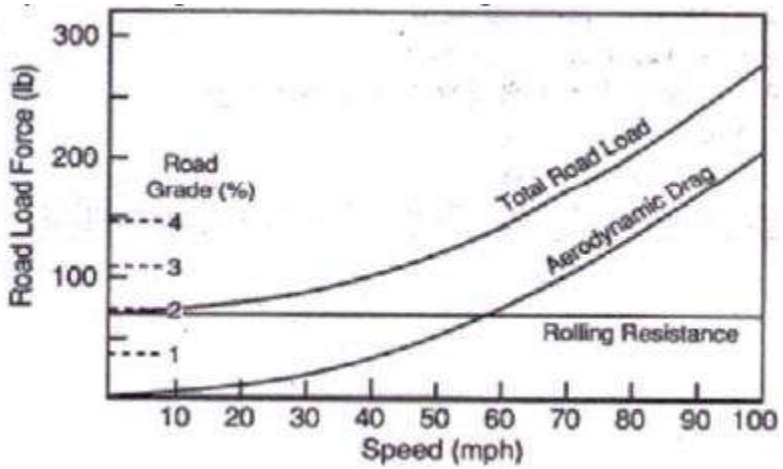

Figure 6 - Correlation between Vehicle Dynamics (Aerodynamics) and Speed (Taherian, 2014)

2.4.2. 85 kWh Battery

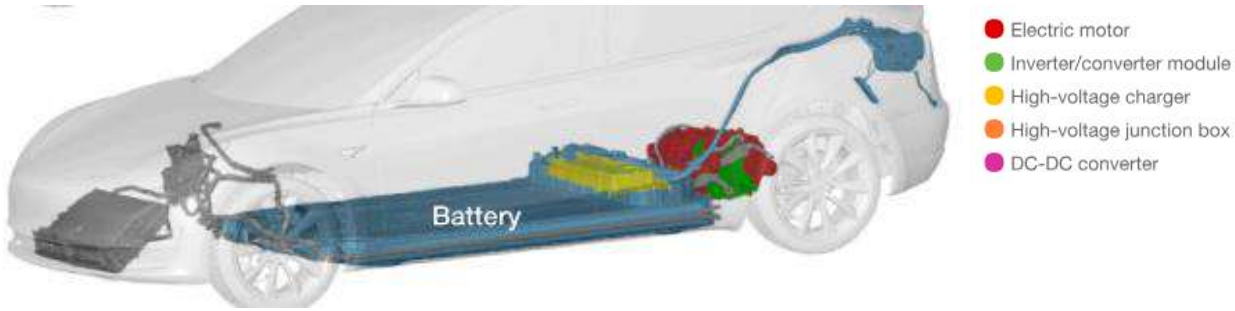

Figure 7 - Battery Pack of Tesla Model S P 85 (Hawley, 2017)

Panasonic manufactures Tesla's lithium-ion graphite batteries. (Hawley, 2017) suggested that the battery pack implemented in Tesla Model S P85 is assembled with 7 104 18650 cells, distributed in 16 modules wired in series, each with six groups of 74 cells wired in parallel, wired in series within the module. The Panasonic batteries used are direct current devices while the domestic services are alternating current (AC) hence, Tesla S P85 uses rectifying converters to convert it to CC which allows the battery to charge reasonably quickly (HYE, 2018). The specific characteristics and features of the battery are mentioned in the '*Methodology'* section, where it is thoroughly evaluated.

The battery would add limitations to the car's performance which would be determined through deriving maximum voltage, current, torque and velocity.

2.4.3. Tesla 3 phase and 4 pole AC induction motor & Brushed DC Motor

Instead of a combustion engine, Tesla Model S comes with an electric motor that converts electric energy into kinetic energy and becomes a source of energy, transmitted to the wheel thus, enabling kinetic movement of the vehicle.

Figure 8 shows the general/overall overview of the Tesla induction motor, obtained from (ARTICLES, n.d.). One of the major areas this article lacked in was to identify the specific motor's specifications; however, it greatly analysed the AC induction motor to gain in-depth knowledge of how AC motor works. Hence, (ATO, 2019)

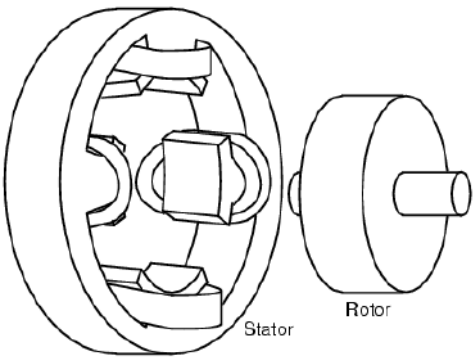

Figure 8 - Tesla Polyphase Induction Motor (ARTICLES, n.d.)

exhibited the relevant characteristics of Tesla's motor needed to carry out the battery analysis.

The actual Tesla S P85 uses three-phase and four-pole AC induction motor, but due to its complexity, it was worth considering brushed DC motor with modified parameters to replicate AC motor performance. The brushed DC motor did not have a significant impact on the function of the vehicle as far as the Simulink model was concerned.

Relevant features of the Tesla AC motors were deduced from (ATO, 2019) and processed further to design a Simulink model for DC motor. (Bakker, n.d.) was used to fully understand Tesla's AC induction motor while also to identify possible ways to effectively demonstrate that DC motor could be used in the Simulink model to function as an AC induction motor. It should be noted that (Bakker, n.d.) did not embody the Simulink model of the DC motor; it simply explained the critical features of AC and DC motors. However, the wiring diagram aspect of the AC induction and DC motors were almost entirely ignored as it did not have a great deal of impact on the Simulink Model.

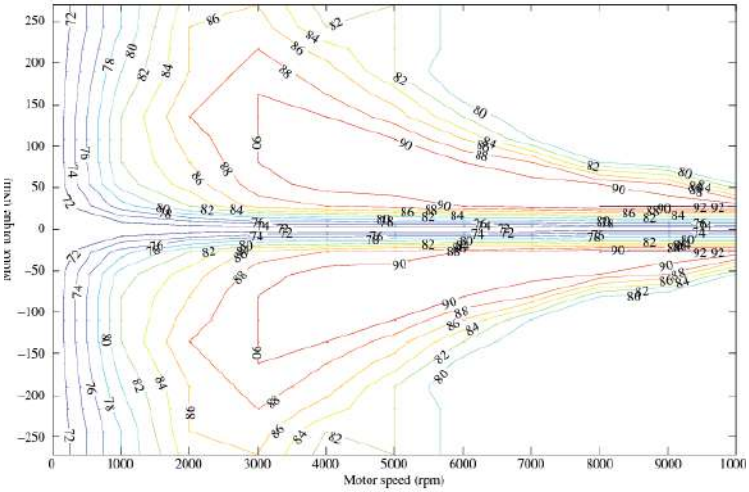

Figure 9 - Efficiency map of AC induction motor

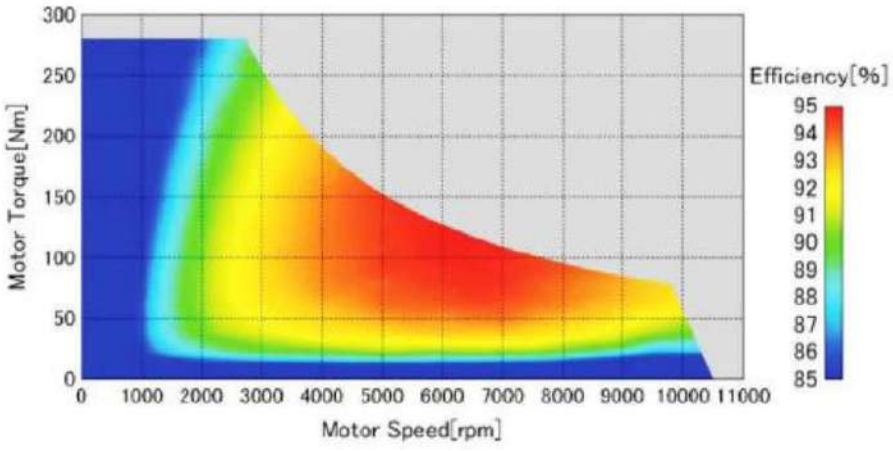

Figure 10 - Mapped Performance of a general AC induction motor with three phase and four poles (jBEAM, n.d.)

The ‘Research and Development’ of motors done by (jBEAM, n.d.) suggested an inverse correlation between motor speed and torque while the efficiency was colour coded as shown in Figure 10. The simple performance mapping done by the author determined motor speed and efficiency. However, the writer did not consider the impact the outside condition had on the efficiency (aerodynamics) but still Figure 10 would be a good benchmark to have while analysing the motor and the vehicle dynamics.

The AC induction motor of Tesla has a three-phase current path that produces mechanical speed or the synchronous speed, expressed by equations shown below. (Engineering Corporation, 2004)

$$n_1 = \frac{60 * f}{p} \qquad eqn.(2.4.3.1.)$$

$$S = \frac{n_1 - n}{n_1} \qquad eqn.(2.4.3.2.)$$

$$T = \frac{3 \times R_2 \times I_2}{s \times n_s} \qquad eqn.(2.4.3.3.)$$

Torque, T of AC motor derived from equation 2.4.3.3. was used to analyse the features and characteristics of the AC motor. The parameters of the DC motor were modified accordingly in the Simulink model.

Figure 9 shows the efficiency map of AC induction motor obtained from (Liu, 2017). Although it does not replicate the very Tesla motor however, it does show the general efficiency of three phase and four pole AC induction motor which would be very close to the one of Tesla. Hence, relevant data were extracted from (Liu, 2017) and translated to the Simulink model to design the DC motor.

2.4.4. Wheels

In simple terms, wheels translate the torque of the motor to a moving force while producing forward or backward friction as it interacts with the asphalt. The effect of wheel wear rate as well as of the tyre pressure on the speed control system was ignored since, firstly it was minute (Muir, 2019) and secondly, insignificant data was available particularly on Tesla tyres to analyse the impact. While also being out of the scope of this report.

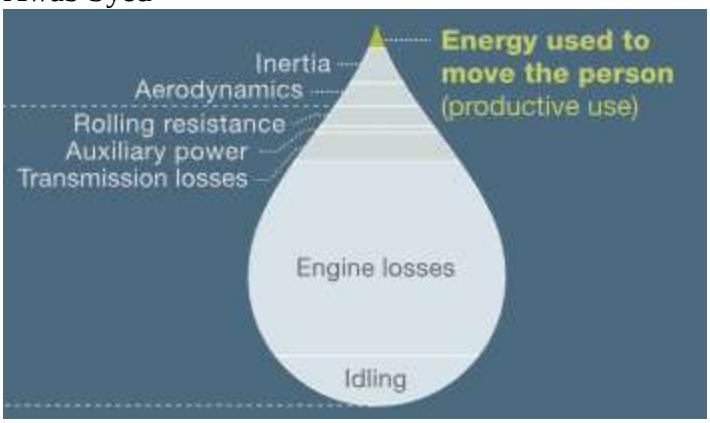

Figure 11 - Transfer of energy/power in Tesla Model S (Mckinsey & Company , 2014)

The analysis done by (Mckinsey & Company , 2014) on Tesla motors categorically stated that '86% of fuel never reaches the wheels' which demonstrated the efficiency of the vehicle. However, the author did not specify the outside condition in which the result was obtained in or the parameters set while research was carried. It was of certain that the speed of the wind and the weather conditions (slope/driving surface) certainly affect the aerodynamics and the rolling resistance respectively. Hence, it was necessary to consider other features (i.e. time it takes to reach 100 km/h) of the car while modelling the vehicle dynamics in order to replicate the actual Tesla S P85.

2.5. Control Systems

Control system is used to modify and monitor the response of the object and also implemented to control the output over a desired period of time. With respect to the speed control system, the controller must be tuned so that the system reaches and maintains the desired speed regardless of the surface, slope, adverse wind and outside condition. (Hill, 2005)

Note that, Figure 12 shows a model for pilot control behaviour extracted from (Hess, 2014). The theory and the concept behind it were very similar to the one of the speed control system. The computer simulation model had used an 'adaptive logic' which allowed the model to have superior performance when compared to the one without it. The author had dwelled with various adaptive logic of equations; however, it was unnecessary to take the

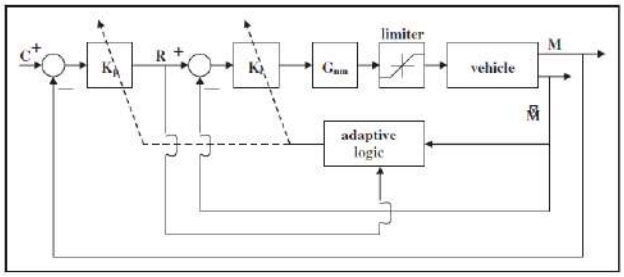

Figure 12 - The adaptive pilot model from (Hess, 2014)

equations route when the MATLAB Simulink instinctively and robotically processes it. Although, a possible reason that could justify (Hess)'s equation approach was the fact that it involved calculating numerous flight conditions. Hess's model was taken into consideration while modelling the closed loop response.

2.6. Control Theory

Control theory deals with the behaviour of the dynamical system to obtain the desired output by manipulating the input. Two foremost categories of control theory; open and closed loop system, in our case, the closed loop response is the main focus as it has a feedback system that regulates, monitors and modifies the output as done by the 'Sensor' in Figure 13. However, the results from the open loop configuration are also crucial to measure the response of the system with no feedback loop (Electronics , n.d.).

2.7. Potential Control Systems

PID controllers consist of three modes; P-proportional, I-integral and D-derivative, while it is possible to construct a closed loop control system using only a single mode, either P or I. However, the integral mode being used all alone is a rare scenario and is not a practical solution to most of the real-life problems as stated by (Mishra, 2014).

P-controller system is typically used for first order processes in linear feedback control systems to stabilise and steady the unstable process i.e. to decrease the steady state error. As the author, (Temel) suggested in the article that P controllers can never be managed to entirely eliminate the steady-state error which meant in respect to the speed/cruise control system that it could not stabilise higher order processes. Though it also causes oscillations, discussed later.

PI controller system is generally implemented to counterattack the steady state error resulted from P controller mode but one of the main downsides of the PI controller is that when the model is highly nonlinear and uncertain, PI controller fails to deliver. Introducing I-integral mode to the P controller also immensely affects the speed and the stability of the system which negatively impacts the oscillations and overshoots the step response. Hence, applying the D-derivative mode, making it a PID controller which could be 'tailored to optimise a particular control system' (Li, 2006). The use of D-derivative mode in the PI controller would eliminate the overshoot and the oscillations occurring in the output while reducing the rise time and improving the stability of the

system. The report written by various intellect including (Li, 2006), (Temel) and (Mishra, 2014) suggested that the PID controller was the optimal controller to design the speed control system.

2.8. PID based Model

$$Standard\ MATLAB\ PID\ Block \qquad K_p + \frac{K_i}{s} + K_d s \qquad eqn.\ 3.8.1.$$

Figure 13 shows a simple 'cruise control' model designed by (Hill, 2005) to regulate the speed of the vehicle. The feedback configuration would loop the output to the controller which could well be the PID with defined parameters. The author did not consider the potential impact the motor efficiency or the traction speed could have on the performance of the overall system. Although, block manipulation technique is used to condense the plant dynamics into a single block for simplification while still providing the very same overall transfer function.

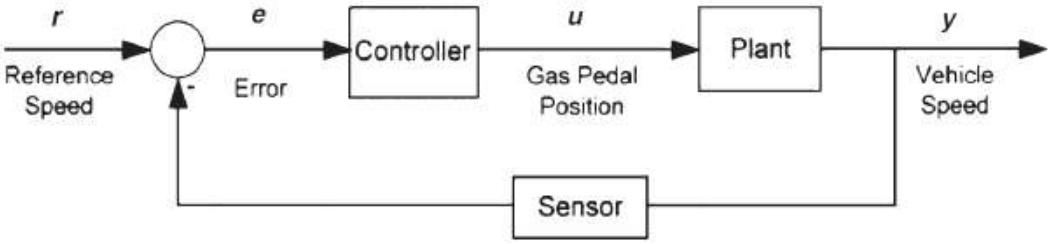

Figure 13 - Feedback control configuration with cruise control (Hill, 2005)

2.8.1. Algorithms – Tuning PID

P-Proportional gain mode controls the response speed of the control system and determines its oscillation frequency (Honeywell, 2000).

$$P = K_p e(t) \qquad eqn.\ 2.8.1.1$$

I-Integral mode sums the error over time and reacts in a particular manner to cause the integral component to increase slowly even with a small error to reach a zero steady-state error (Hogenson, n.d.).

$$I = K_i \int_0^t e(\tau) d\tau \qquad eqn.\ 2.8.1.2.$$

D-derivative mode causes the output to decrease if the process variable is increasing at a rapid pace. Derivative time (Td) controls the sensitivity of the control system, making it react more vigorously or languorously depending on the input Td (P567).

$$D = K_d \frac{de(t)}{dt} \qquad eqn.\ 2.8.1.3.$$

One of the most important and surprising concepts (Liu, 2017) used in his model is the anti-wind-up function which accounted for the microscopic nonlinear effects i.e. the fact that the traction speed of the motor has a limit.

From the simulating point of view, once the desired output is achieved, the feedback loop is broken, and the model goes into an open loop configuration. Hence the control error is continuously integrated, and action is accumulated, it affects the quickness of the PID algorithms to return to normal. Therefore, the author attempted to resolve the control system by implementing an anti-wind-up function that prevented integration (I-integral) wind-up in PID controllers. Additional necessary research was obtained from (K. Astrom, 2005) to thoroughly analyse and implement it to the speed control system designed on MATLAB Simulink.

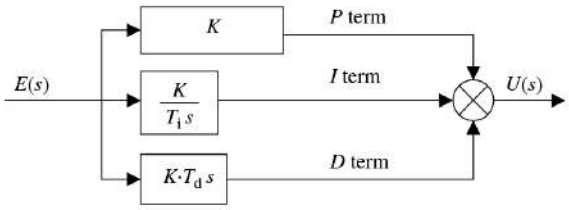

Figure 14 - Block diagram of a PID control algorithm (Hill, 2005)

Method	Advantages	Disadvantages
Manual	Online method No math expression	Requires experienced personnel
Ziegler-Nichols	Online method Proven method	Some trial and error, process upset and very aggressive tuning
Cohen-Coon	Good process models	Offline method Some math Good only for first order processes
Software tools	Online or offline method, consistent tuning, Support Non-Steady State tuning	Some cost and training involved
Algorithmic	Online or offline method, Consistent tuning, Support Non-Steady State tuning, Very precise	Very slow

Figure 15 - Possible tuning methods for PID Controller used for speed control system (Mpanda)

Variety of PID tuning methods are shown in Figure 15 including 'Ziegler Nichols Design Method', 'Trial and Error method', 'Cohen Conn'.

The in-depth analysis done by (Mpanda) shown in Figure 15 exhibits the possible tuning approach for the speed control system. However, the author did not analyse nor evaluate the built-in automatic tuning feature in MATLAB. This feature is explored in the 'Methodology' section of the report.

	Rise Time	Overshoot	Settling Time	Steady-State Error	Stability
Increasing K_P	Decrease	Increase	Small Increase	Decrease	Degrade
Increasing K_I	Small Decrease	Increase	Increase	Large Decrease	Degrade
Increasing K_D	Small Decrease	Decrease	Decrease	Minor Change	Improve

Figure 16 - Effects of independent P, I, D tuning on closed-loop response. While K1 and KD are fixed, increasing KP alone can decrease rise time, increase overshoot, slightly increase settling time, decrease the steady state error, and decrease stability margins. (Li, 2006)

2.8.2. Interpreting Control System Response and Terminology

It is essential to know how to approach the results obtained from the Simulink model and to understand the basic terminologies of MATLAB. The detailed explanation on PID interpretation done by National Instruments known for manufacturing automated equipment (National Instruments , n.d.) was considered. However, the system used in the journal was not related to speed control system but the approach towards the data obtained from the Simulink model would be the same.

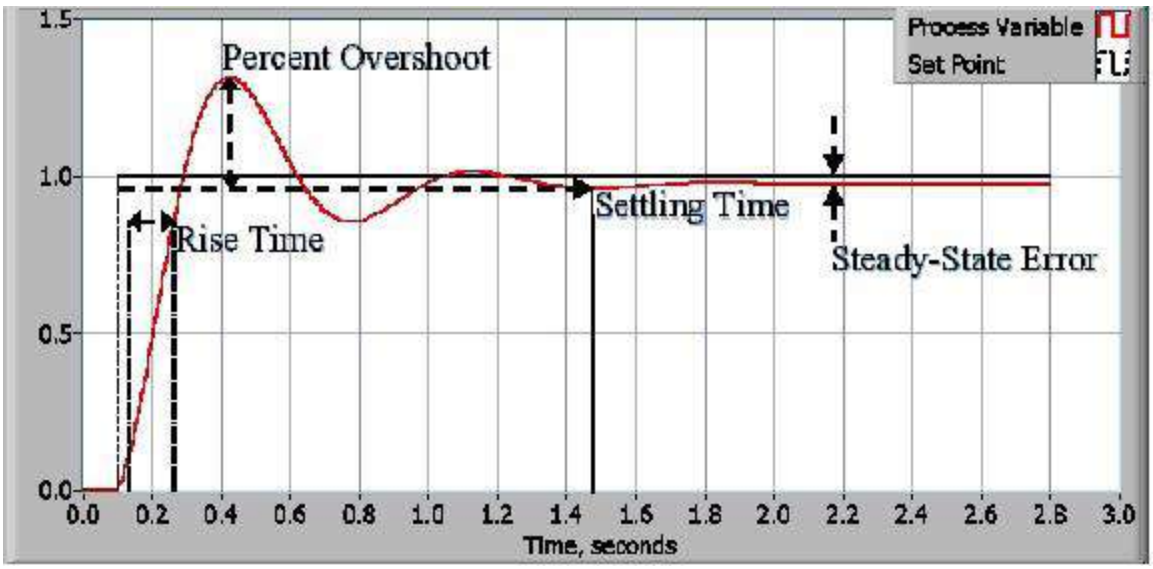

Figure 17 - Response of a typical PID controller (National Instruments , n.d.)

Figure 17 depicts a typical response given by a PID controller implemented in a control system. The terminologies would be used to develop the system parameters or the performance criteria for the speed control system.

3. Methodology

3.1. Mathematical Model / Vehicle Dynamics

The mathematical model was constructed and used as the basis to design the model on MATLAB Simulink. The general characteristics and specs of the Tesla Model S P85 were extracted from the automobile database (Tesla - Model S - P85 PERFORMANCE (416Hp)) and compared against other reliable sites and article (Cain, 2014) due to the fact that there were significant modification/variation amongst the same model of different year release. These characteristics are shown in section '*2.4: Tesla S P85 Vehicle Dynamics'* of the report. The model of 2013 was selected once in-depth research was carried out since it is a model that has the least modification.

Selecting more recent models of S P85 would simply make the mathematical model and the Simulink representation much more complex while adding little to no significance to the main objective of the report, the implementation of the control system.

One of the major noticeable alterations between 2013 (P85) and the 2018 (P 85D) model was that the recent ones were accommodated with two motors, making it an all-wheel drive (AWD). This allowed better traction control which would be beneficial in the snow-prone region of the world. There were other potential benefits of it however, it was out of the scope of this report. Hence, the 2013 model of S P85 was selected as it met the set objectives while avoiding any unnecessary complexity.

Figure 18 shows the Simulink model from an aerial view; this allowed to gain a general overview of the way the vehicle interacts with the speed control system as well as the interactions between each component. The speed applied through the pedals of the vehicle was the 'Input' voltage which was limited due to the performance of the battery i.e. the maximum voltage the battery was capable of producing. The voltage produced by the battery was applied to the DC motor, causing a forward force. External vehicle dynamics, i.e. the resistance caused by the air hindered or worked against the forward force. This was implemented in Simulink by determining 'work efficiency' of the vehicle so that the model reached 100 km/h within 4.4 seconds as in real life.

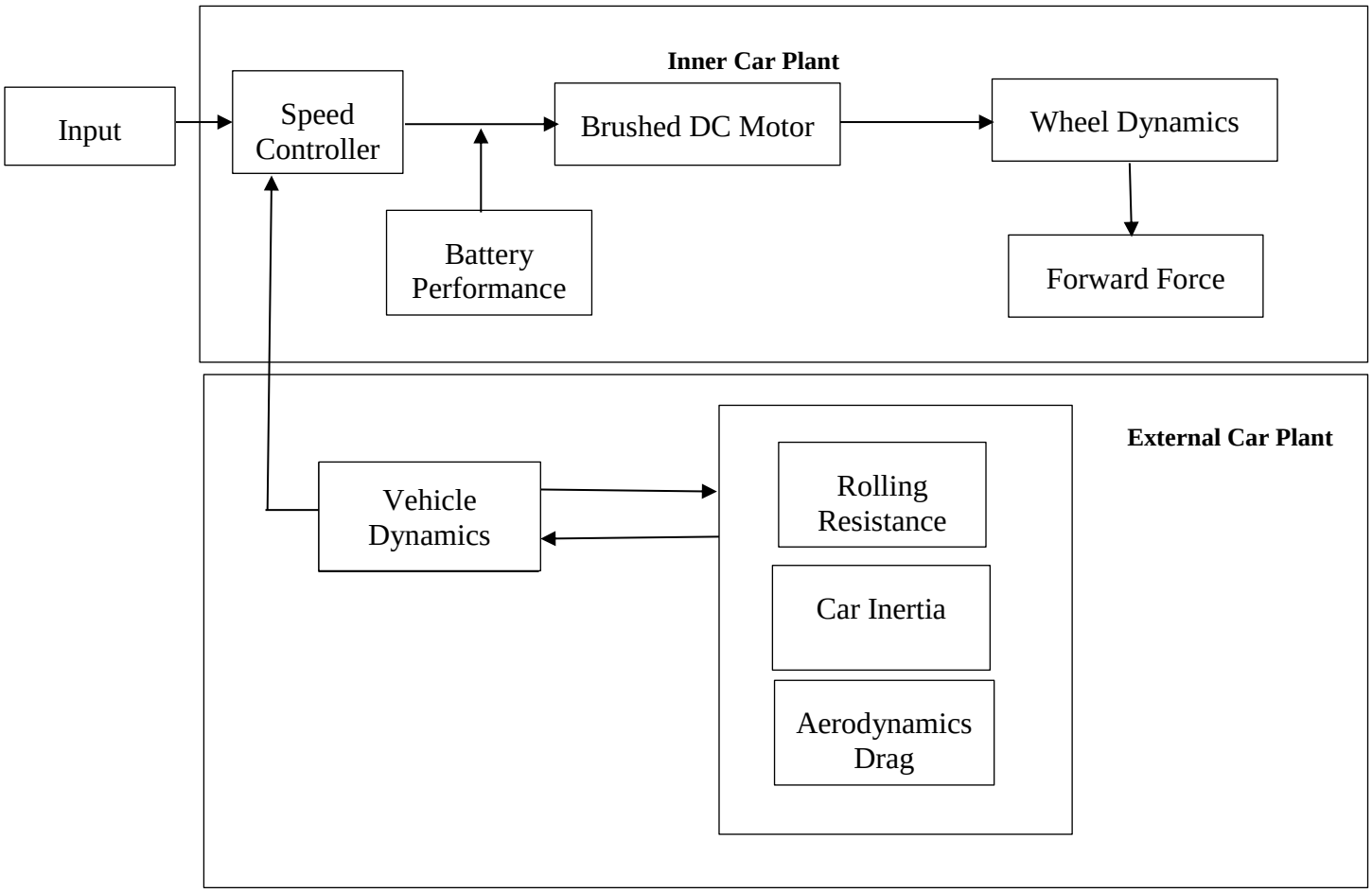

Figure 18 - Shows the overview of the Simulink model

3.1.1. Battery

The internal structure of the battery was discussed and concluded in the literature review section '*2.4.2. 85 kWh battery'*, briefly be summed as:

- Assembled with 7 104 18650 Lithium-ion cells
- 16 Modules wired in series, each containing six groups of 74 cells wired in parallel themselves wired in series within the module
- Total capacity = 85 000 Wh
- Weighs 540 kg
- Each NCR18650B cell has an average capacity of 3300mah, a nominal voltage of 3.6V, about 11.9Wh
- Maximum voltage is 4.2V, discharge at 2.5V

In a parallel circuit arrangement, the voltage remains the same throughout the circuit while the current is distributed between each branch. Hence the nominal voltage was calculated using equation 3. 1. 1.1. as shown below.

$$V_{Nominal} = Nominal\ voltage\ \times No.of\ Modules \times No.of\ sections\ (groups) \qquad eqn.\ 3.1.1.1.$$

$$V_{Nominal} = 3.6 * 16 * 6 = 346V$$

The data from (HYE, 2018) was used to derive equation 3.1. 1. 1. to obtain a nominal or mean voltage of 346V which was also assumed to be the maximum operating voltage of the battery.

Assumption: It was assumed that the voltage of the battery stayed constant with the maximum voltage of 346V which limited the discharge rate of the battery. However, it was possible to track the total discharge capacity/rate and scale the battery voltage accordingly, but it would make the model much more complicated without serving any real benefit as the focus of the report was mainly on the speed control system and modelling Tesla.

Since torque produced by the motor was proportional to the gain in current by the motor, the maximum torque was used in amalgamation with the proportional constant to calculate the maximum current going through the battery. This is explained in-depth later on in the report, it is briefly mentioned here as it affects the performance of the battery.

NOTE: All these parameters and assumptions will be appropriately implemented in Simulink MATLAB.

3.1.2. Motor

As stated in the literature review section '*2.4.3. Tesla AC 3 phase and 4 pole induction motor',* the vehicle; Tesla S P85 is equipped with three-phase AC four pole induction motor which would be replicated using brushed DC motor with modified parameter/characteristics in the Simulink model. The performance of the modified DC motor would be similar to the actual Tesla S P85 motor as deduced in the literature review. Both; AC Tesla motor and the DC electric motor converts electricity into motion however, AC is much more efficient in the practical world since it minimises mechanical losses but as far as this particular Simulink model is concerned, using brushed DC motor would not affect the performance.

Assumption: Low state of charge and the cold outside temperature can potentially reduce the flow of the electron below the ultimate capabilities of the electric motor. However, throughout the mathematical and Simulink model, it was assumed that it did not have any effect on the performance of the motor. Hence, it was ignored. This was mainly because it would require an immense amount of primary and secondary data, to derive its impact while it was out of the scope of this report.

Figure 19 depicts the brushed DC motor circuit on which Ohms' and Kirchhoff law was implemented to obtain the torque generated by the motor through calculating voltage and EMF.

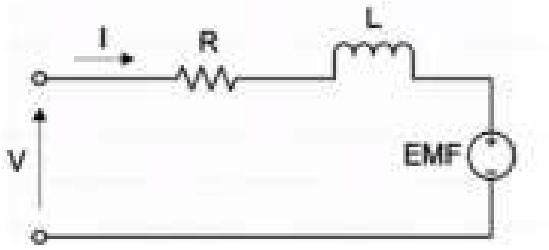

Figure 19 - Circuit representing the brushed DC motor (Engineeringtoolbox , n.d.)

$$Ohms'Law \qquad V = I * R \qquad eqn.\ 3.1.2.1.$$

$$Inductance\ Equation \qquad V = L * \frac{dI(t)}{dt} \qquad eqn.\ 3.1.2.2.$$

$$Kirchoff's\ voltage\ law \qquad V = I(t) * R + L\frac{dI(t)}{dt} + E(t) \qquad eqn.\ 3.1.2.3.$$

Implementing Kirchhoff's voltage law to the circuit shown in Figure 19, "*the sum of all voltages across a closed path in a circuit is equal to zero*". (Electronicstutorials, n.d.). Ohm's law and inductance equation were substituted into Kirchoff's voltage law to obtain equation 3.1.2.3.

Electromotive force, E(t) with respect to time is the voltage generated by the brushed DC motor; hence, the equation 3.1.2.3. represents the motor.

$$Torque\ (Motor) \qquad T(t) = K_T * I(t) \qquad eqn.\ 3.1.2.4.$$

$$Back\ EMF\ (Motor) \qquad K_E(t) = K_E * \omega(t) \qquad eqn.\ 3.1.2.5.$$

$$K_T * I(t) = j \times \frac{d\Omega}{dt} \qquad eqn.\ 3.1.2.6.$$

Where; j = moment of inertia of the motor

$$Brushed\ DC\ Motor \qquad V(t) = I(t)R + \frac{LdI(t)}{dt} + K_E\omega(t) \qquad eqn.\ 3.1.2.7.$$

Brushed DC motor equation (eqn. 3.1.2.7.) shown above was obtained through transposing and substituting inductance and back EMF equation into the Kirchhoff's voltage law.

$Laplace\ Domain\ \ (Motor)$ $V(s) = R * I(s) + sLI(s) + K_E\omega(s)$ $eqn.$ 3.1.2.8.

$Laplace\ Domain\ (Torque)$ $T(s) = K_T + I(s)$ $eqn.$ 3.1.2.9.

Applying Laplace domain to the brushed DC motor and to the torque equation resulted in equation 3.1.2.8 and 3.1.2.9 which would be implemented in the MATLAB Simulink. The Laplace domain (torque) equation represents an electric DC motor which would with precise parameter depicts the Tesla AC induction motor (Bissell, 1988).

NOTE: Full working for Laplace transformation is not shown due to space constraint.

$Transfer\ Function$ $I(s) = \frac{V(s) - K_E * \omega(s)}{sL+R}$ $eqn.$ 3.1.2.10.

Rearranging Laplace domain (motor) equation to obtain a transfer function by making current; I(s) that goes through the DC motor, the subject.

$Torque\ Function\ of\ voltage$ $T(s) = K_T * \frac{V(s) - K_E * \omega(s)}{sL+R}$ $eqn.$ 3.1.2.11.

Linking voltage directly to the torque generated by the motor, so that a transfer function could be used, where voltage is an input while torque is an output

Through observing equation 3.1.2.11., it was deduced that the numerator referred to the voltage the motor was experiencing. In other words, the motor not only experienced the voltage applied from the accelerator(pedals) but also the voltage generated by the motor itself due to its rotation. Hence, the voltage experienced by the motor is the voltage applied minus the electromotive force generated by the motor itself.

Specific system parameters of Tesla S P85 was extracted from section '*3.3'* and inserted into equation 3.1.2.11. It gives torque output as a function of rotational velocity and the voltage applied to the motor as illustrated in the equation below.

$Mimics\ Tesla\ AC\ Motor$ $T(s) = 0.25 * \frac{V(s) - 0.12 * \omega(s)}{(493 * 10^{-9}s) + (5.3 * 10^{-3})}$ $eqn.$ 3.1.2.12.

Equation 3.1.2.12. defined the parameters and the characteristics of the brushed DC motor which mimics the performance of the Tesla 3 phase AC four pole induction motor. This was an essential equation that would be used immensely to construct the Simulink Model as it replicated Tesla motor.

Tesla S P85 has a gear ratio of 9.73 which suggest that the actual rotational velocity fed back to the system must be scaled accordingly. Hence, the wheels spin 9.73 slower than the motor due to the gear ratio.

NOTE: Inverse Laplace and time domain was not considered as MATLAB Simulink has a built-in feature for it. The mathematical model was limited to the Laplace domain.

3.1.3. Traction Force

Relevant wheel dimensions of Tesla S P85 was extracted from the literature review section and are as follows;

- Radius – 0.24 m
- $L_R = 24\ cm$
- $Circumference = 2\pi r$

The circumference was used to calculate the angular velocity of the wheel from the forward velocity of the car.

Figure 20 - Wheel design of Tesla Model S P85 (Lambert, 2018)

Assumption: The reduction in the radius of the tyres was ignored simply because it was out of the scope of this report. However, in reality, the radius would vary slightly due to compression under weight, since it is made up of rubber and inflated with air. Though, this would slightly be compensated with the overall efficiency of the vehicle which is covered in the later section of the report.

The torque produced by the motor is transmitted to the wheels to generate forward force. This was expressed in the equation below.

$$Traction\ Force \qquad F_f = \frac{T}{L_R} * R_g \qquad eqn.\ 3.1.3.1$$

$$Where; L_R = \frac{D}{2} = \frac{48}{2} = 24\ cm$$

$$\therefore F_f = 40.5T \qquad (Where\ G_r = 0.93)$$

Assumption: In the practical world, 'slip' occurs between the wheels and the surface which would have an impact on the forward /traction force as well as on the friction. The level of 'slip' depends

on the surface; however, the impact of 'slip' was not considered in this report. The impact was limited and had a slight impact on the acceleration of the vehicle.

3.1.4. Aerodynamic Drag

Aerodynamic drag occurs between the shell of the vehicle and the air when moving (displaced). There are two forms of aerodynamic drag; friction and pressure drag. Friction drag are caused by the air molecules rubbing at the shell of the car while pressure drag occurs when the air is displaced around the vehicle. Hence, drag force (D_F) was calculated through the following formulae:

$$D_F = \frac{1}{2}\rho V^2 A C_D \qquad eqn.\ 3.1.4.1$$

$$Where; A = Frontal\ Area$$

Assumption: Vehicle was at Sea level $\therefore Density = 1.225 kg/m^3$

Other values were extracted from the section;'*3.3. System Parameters'* and were used to derive equation 3.1.4.1

$$D_F = \frac{1}{2} 1.225 * v^2 * 2.34 * 0.24$$

$$\therefore D_F = 0.3381 v^2 \quad Where; v = velocity$$

The drag force of the Tesla Model S P85 calculated above was relatively low compared to other electric vehicles due to the shape/design of the car.

3.1.5. Rolling Resistance

Rolling resistance occurs at the interaction between the vehicle's wheels and the surface due to the absorption of energy by the tyre.

$$F_R = C_R * m * g \qquad eqn.\ 3.1.5.1$$

$$F_R = 0.02 * 2108 * 9.81$$

$$\therefore F_R = 413\ N$$

Assumption: The driving surface was Asphalt/Bitumen

3.1.6. Motor Traction

Motor traction is the only force that drives the vehicle forward while the aerodynamic drag and the rolling resistance act in the opposite direction. Motor traction of the Tesla S P85 was calculated using the traction force (F_f) and the overall efficiency of the car.

At this point in the report, the overall efficiency of the car was unknown. However, it was obtained from the Simulink model shown in section *'3.6. Closed Loop Response'.* To attain the efficiency of the vehicle, parameters such as the time it took the model to reach 100 km/h was used while reverse engineering was applied to the result obtained. It was deduced that the car had an overall efficiency of 60% (0.6) since the car reached 100 km/h within 4.4 seconds which is the actual time for the Tesla S P85.

The overall efficiency calculated takes into account all the mechanical losses/inefficiency i.e. heating of components, friction between components as well as the aerodynamic and rolling resistance.

$$Motor\ Traction \qquad M_T = F_f * Overall\ Efficiency\ of\ the\ car \qquad eqn.\ 3.1.6.1.$$

$$M_T = 40.5T * 0.6$$

$$\therefore M_T = 24.3T$$

Motor traction obtained above was used to construct the vehicle dynamics in the Simulink Model.

3.1.7. Applying Newton's Second Law

Newton's second law of motion states '*the acceleration of an object is directly proportional to the net force and inversely proportional to its mass'* (University of Cambridge., n.d.).

$$Newton's\ Second\ Law \qquad \sum F = ma \qquad eqn.\ 3.1.7.1.$$

$$M_T - F_R - D_F = ma$$

$$0.7 * 40.5T - 413 - 0.3381v^2 = ma = 2108 * a$$

$$Plant\ Dynamics \qquad \frac{0.6 * 40.5T - 413 - 0.3381v^2}{2108} = \frac{dv}{dt} \qquad eqn.\ 3.1.7.1.$$

3.1.8. Summary

Two main equations obtained from the mathematical model which would be implemented in the Simulink Model are as follows:

Mimics Tesla AC Motor $$T(s) = 0.25 * \frac{V(s) - 0.12 * \omega(s)}{(493 * 10^{-9} s) + (5.3 * 10^{-3})}$$ *eqn.* 3.1.2.12.

Plant Dynamics $$\frac{0.6 * 40.5T - 413 - 0.3381v^2}{2108} = \frac{dv}{dt}$$ *eqn.* 3.1.7.1.

3.2. Mathematical Model of PID Controller

The mathematical algorithm of the PID controller is represented as:

$$u(t) = K[e(t) + \frac{1}{T_i}\int_0^t e(\tau)d\tau + T_d\frac{de(t)}{dt}]$$ *eqn.* 3.3.1

The control signal, u(t) is the sum of three modes; P- proportional gain, I- integral and d- derivative mode. These were fully analyzed and explained by (Astrom, 2002) in his journal on 'Control Systems'. The textbook algorithm of PID controller shown in equation 3.3.1 would be extrapolated to implement a PID speed control system in the Simulink Model.

The mathematical model of PID transfer function and the closed loop transfer function was considered since the MATLAB Simulink is capable of automatically executing the function.

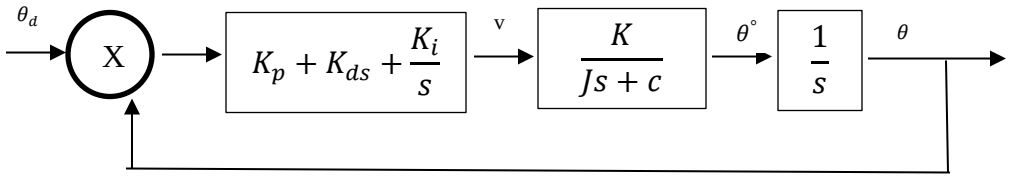

Figure 21 - Simplified mathematical model

$$\theta = \left[\frac{K(K_p + K_{ds})}{s(Js + c)}\right](\theta_d - \theta)$$ *eqn.* 3.3.2

$$\theta\left[1 + \frac{K_pK + K_dK_s}{Js^2 + cs}\right] = \left(\frac{k\,K_p + k\,K_ds}{Js^2 + cs}\right)\theta_d$$

$$\frac{\vartheta}{\vartheta_d} = \frac{k\,K_d + k\,K_ds}{Js^2 + (c + k\,K_d)s + K_pk}$$

3.3. System Parameters

Weight: 2, 108kg

Drag Coefficient C_D: 0.24

Fontal Area: $2.34m^2$

100 km/h = 4.4 seconds

Torque: 600Nm @ 0RPM

$C_r = 0.02$

Maximum Velocity: 250 km/h

Power: 416 HP / 310kW @8,600 RPM

Wheel Rolling Resistance Coefficient on Asphalt: 0.02

Battery Capacity: 85 kWh

Gear Ratio: 9.73 to 1

NOTE: These specifications were extracted from (Cain, 2014) and (B, n.d.)

Data obtained from online article/forum (B, n.d.) / (Tesla - Model S - P85 PERFORMANCE (416Hp)) / (Kenny, 2015) / (Chen-Yu-Hsieh, 2014)

$R = 5.3 * 10^{-3} \Omega$

$L = 493 * 10^{-9} H$

$K_E = 0.12 V_s/rad$

$K_T = 0.25 Nm/Amp$

b = 1138 N.s/m

$R_r = 413 \Omega$

3.3.1. Performance Specifications

Rise Time < 15 seconds

Overshoot < 10%

Settling Time 15 - 20 seconds

Steady State Error < 1%

Stability - The error variable must converge to a small number, ideally zero

Common goals while tuning the controller using various algorithms was summarised as having:

- Fast rise time
- Minimal Overshoot
- Zero steady-state error
- Minimal Settling time

The optimal parameter for the speed control system was deduced from the literature analysis done on PID which would be used to tune the control system. A rise time of less than 15 seconds was in the mid-range, not making the passenger feel uncomfortable through a rapid increase in the speed while at the same time it was not too slow to cause serious delays. Furthermore, a maximum overshoot of 10% with a settling time of 15 – 20 seconds would provide stability to the model.

3.4. Modelling Brushed DC Motor

3.4.1. Block Model

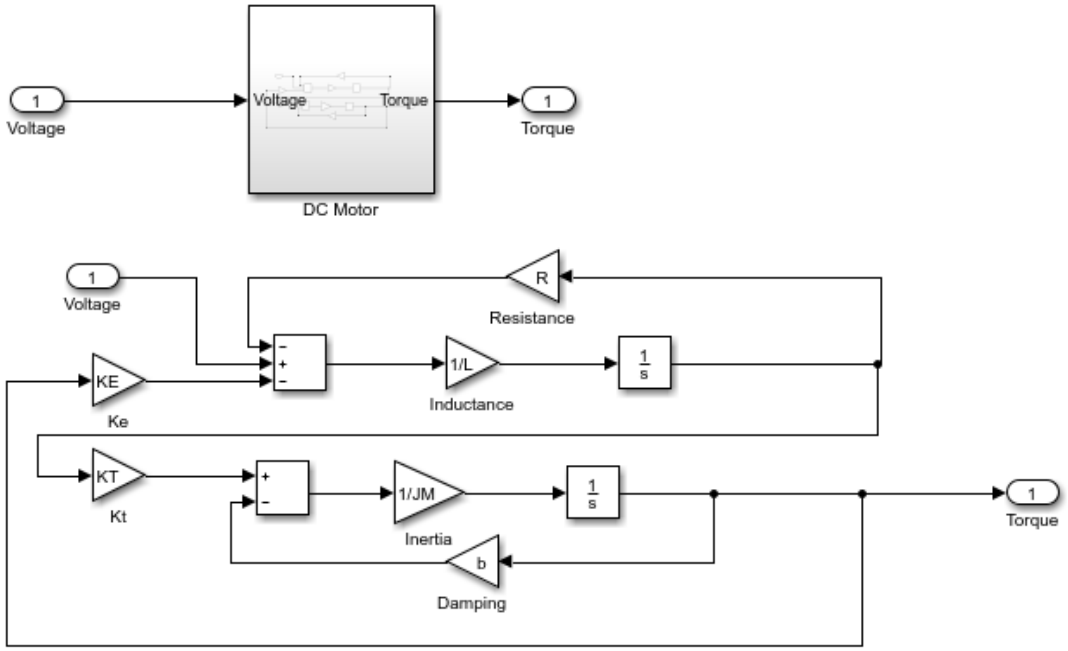

Figure 22 - Block Model replicating the Tesla Motor

NOTE: Figure 58 in the Appendix shows the physical parameters of the block model.

3.4.2. Mathematical Model

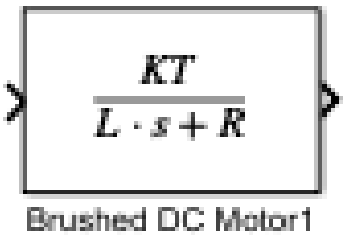

Figure 23 - Mathematical Model of the Tesla Motor

Equation 3.1.2.12. was transferred into the MATLAB Simulink to design a brushed DC motor.

NOTE: Figure 58 in Appendix C shows the physical parameters of the mathematical model.

Two different approaches, mathematical and block model were considered to model the 'Brushed DC motor' that replicated the actual AC induction motor of the Tesla S P85. Both methods considered the actual parameters of the motor and were equally correct. However, the mathematical model was used since it took into account much more realistic parameters and was supported by the mathematical equations.

3.5. Modelling Car Dynamics

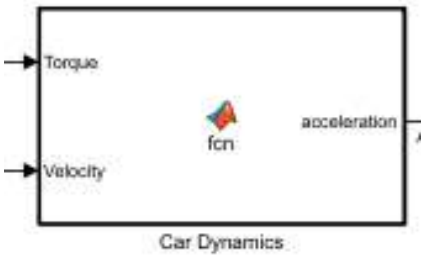


```
function acceleration = fcn(Torque, Velocity)
acceleration = (40.5*Torque*0.6-413-0.3381*Velocity^2)/2108;
```

Figure 24 - Tesla Model S P85 Vehicle Dynamics

$$Accerleration = \frac{M_T * D_F * v^2}{m} \qquad eqn.\ 3.5.1.$$

A special 'user define MATLAB function' was used to model the vehicle dynamics replicating the Tesla S P85.

3.6. No Limitation on Battery (Current)

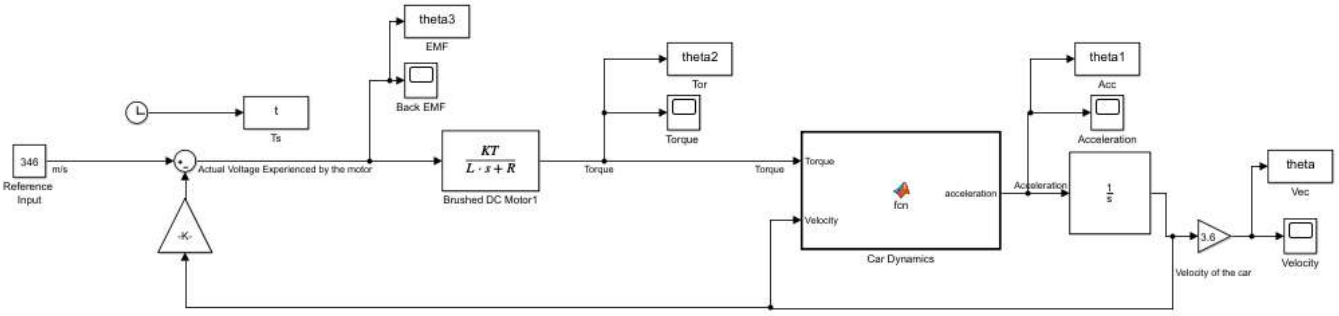

Figure 25 - No limit on the rate of current displaced out of the battery

NOTE: The m-file is shown in Appendix C which was used to construct all the Simulink Model in this report.

3.7. Open Loop Response

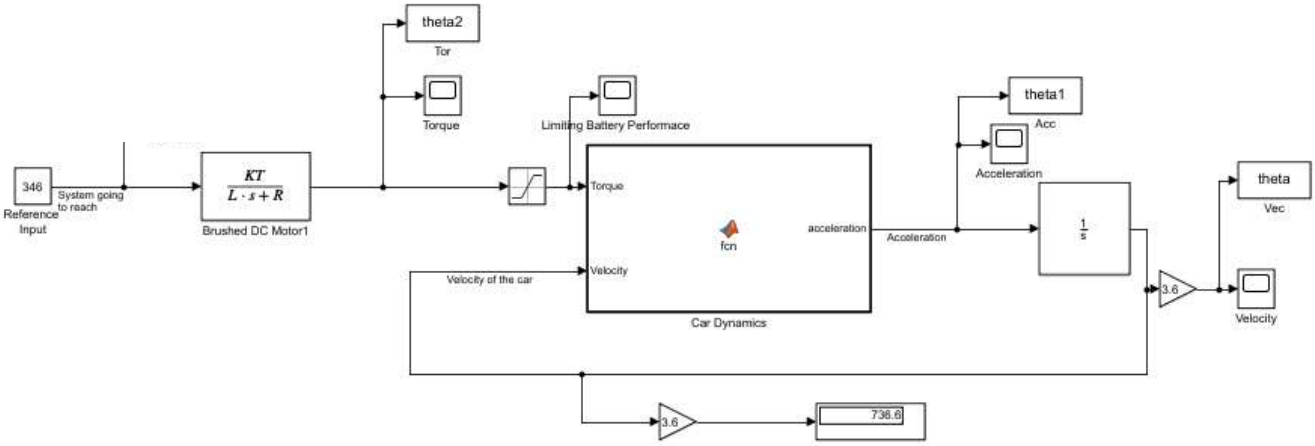

Figure 26 - Open Loop Simulink Model

The open loop model shown above was used to measure the output with no feedback loop which would help to analyse the response of the system. While the open loop model was also used to limit the battery performance to cap the torque produced by the motor.

Figure 27 displays the parameters of the 'Saturation' block used to limit the torque hence, limiting the current, the motor can withdraw from the battery. An upper limit of 600Nm was applied since that is the maximum the Tesla S P85 can reach in the real world as stated in section '*3.3. System Parameter'*.

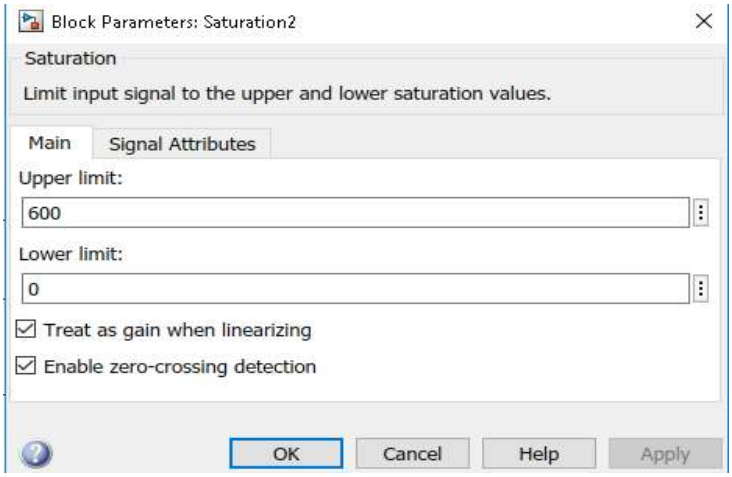

Figure 27 - Shows the parameters of the 'Saturation' block used

3.8. Closed Loop Response

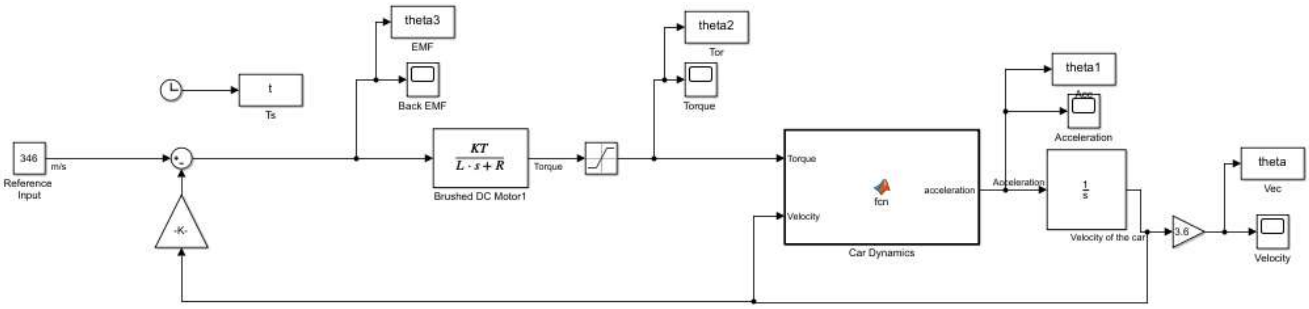

Figure 28 - Closed Loop System

NOTE: m-file shown in Appendix C was used to construct and run the Simulink. The closed-loop system model was used to determine the overall efficiency of the vehicle (*'4.1. Trial and Error Method')* and to ensure that the system response was well-aligned and represented the actual Tesla S P85 before delving into control systems.

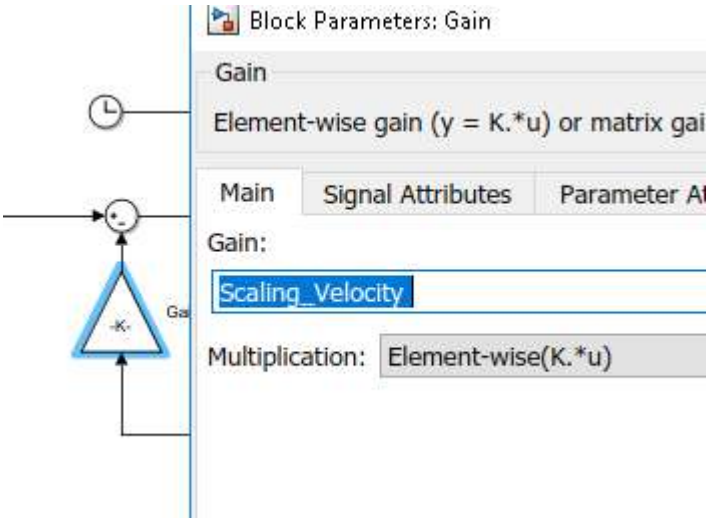

Figure 29 - Parameter of the gain used in the feedback loop. Actual value in m-file shown in Appendix C

The initial rotational velocity of the motor was fed back from the output of the system using a feedback loop. This meant that the system did not have the rotational velocity in the first iteration. It was calculated in the first iteration and given back to the system.

```
>> plot (t,theta); grid;
xlabel ('Time (s)');
ylabel ('Velocity (km/h)');
>> hold on; plot (t,theta,'r'); grid; hold off;
>> hold on; plot (t, theta, 'g'); grid; hold off;
```

Figure 30 - Command used to plot the efficiency graph shown in section 'Trial & Error Method'

3.9. Control System – P, PI & PID

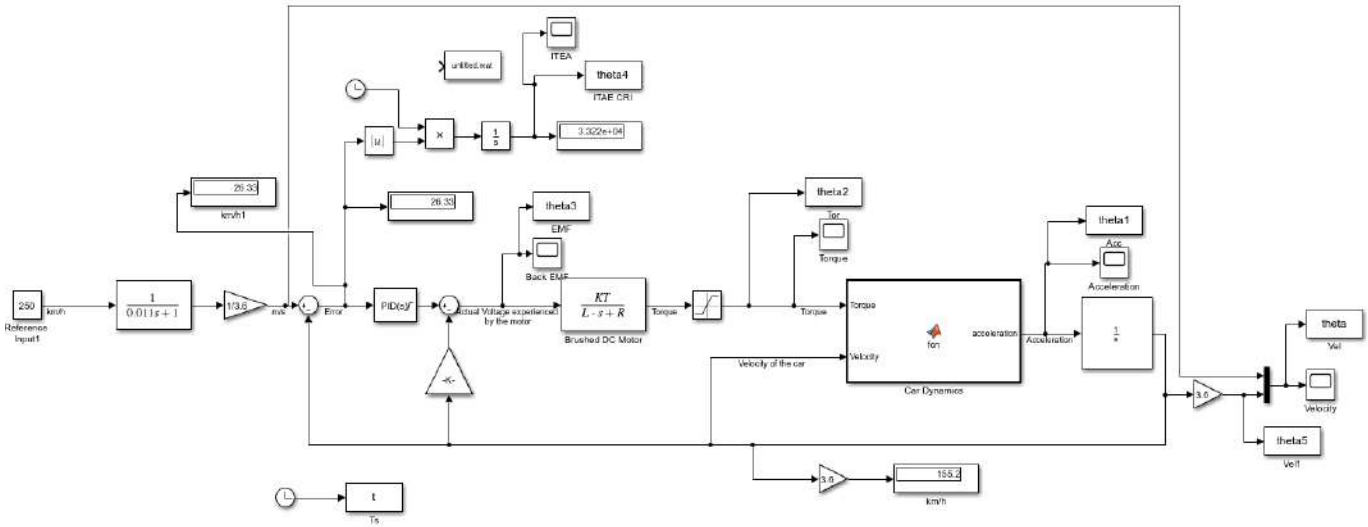

Figure 31 - Shows the Simulink Model with the control system implemented

Figure 31 shows the final model with the speed control system implemented through the *'PID Block Function'* in the MATLAB which represented P, PI and PID controllers depending on the parameters set. ITEA criterion was also implemented in the Simulink model shown in Figure 31 however, it was not used to analyse the system. ITAE analysis formed the part of the '*Further Work'* section.

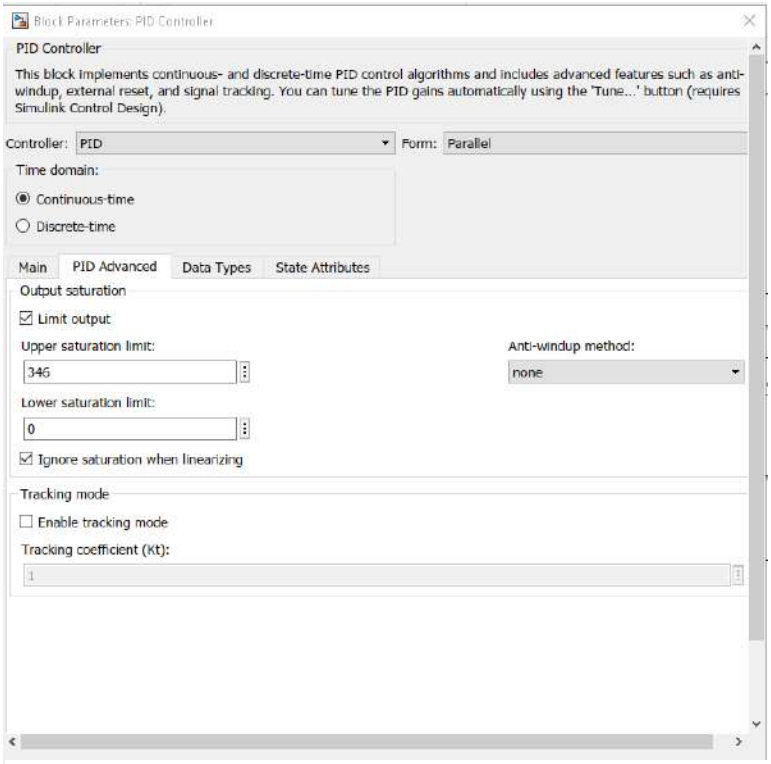

Figure 32 - General parameters of the control system (P, PI & PID)

Figure 32 depicts the general parameter which was constant for all the controllers used in this report. An upper saturation limit of 346V was placed, illustrating the maximum voltage that the battery can displace.

Figure 33 shows the general parameters; P-proportional, I-integral and D-derivative, of the *'PID Block Function'* used in the Simulink model.

To implement the P controller, only P-proportional was tuned while for PI, P-proportional and I-integral were tuned. Lastly for PID, all three; P, I and D-derivatives were tuned using the algorithms defined in the '*Literature Review'* section.

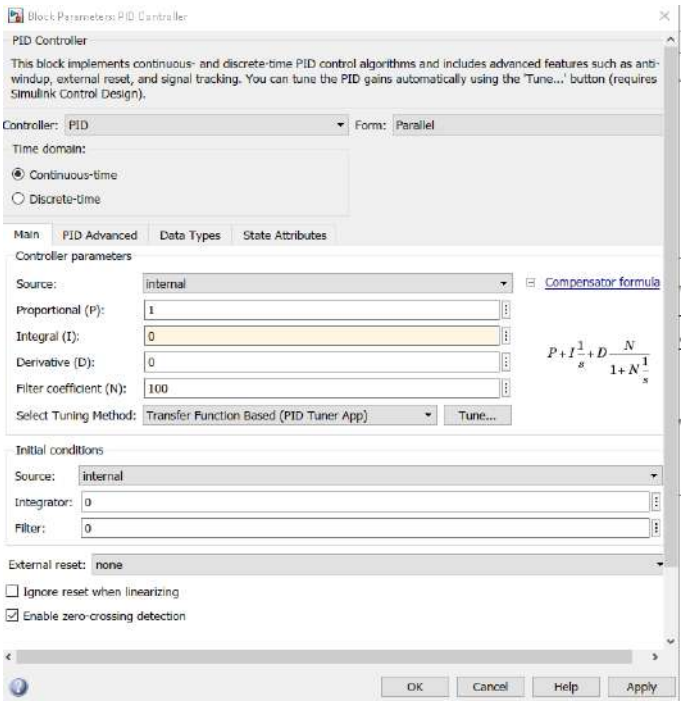

Figure 33 – shows the parameters that would be modified depending on the controller applied

3.9.1. Manual/Heuristic Fine-Tuning (Inspired by Ziegler Nichols Design Method)

A simple approach was taken by keeping I-integral and D-derivative to zero and constructing a P-proportional controller.

$$P - Controller \qquad F_{error} = K_p(e_t) \qquad eqn.\ 3.9.1.1.$$

	k_p	T_i	T_d
P-control	$0.5k_p^*$	∞	0
PI-control	$0.45k_p^*$	$\frac{T_p^*}{1.2}$	0
PID-control	$0.6k_p^*$	$\frac{T_p^*}{2}$	$\frac{T_p^*}{8}$

Figure 34 - Design rule of Ziegler Nichols Design Method (Msstarlabs, n.d.)

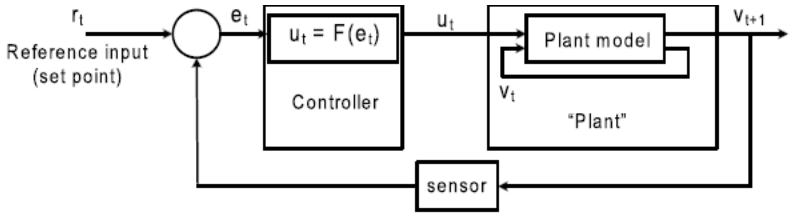

Figure 35 - Referred to during the calculation process

Figure 35 was obtained from one of the journal articles used in '*Literature Review'* to carry out the following calculations.

$$Error = r_t - v_t$$

$section$ 3.1.3. $Where;\ M_t = 24$

$$v_{t+1} = 24v_t + 0.5k_p(r_t - v_t) + dt$$

$$v_{t+1} = (24 - 0.5K_p)v_t + 0.5K_p r_t + dt$$

$$|\propto = 24 - 0.5K_p| < 1$$

$$'If\ that\ is\ the\ case\ then\ v_t\ grows\ within\ bound'$$

$$\therefore K_p > 23.5$$

The P-proportional gain should be greater than 23.5 which was used to determine the gain for the P-controller. This was used to obtain the results shown in section 4.5.1. which was then processed further to derive I-integral gain and later D-derivative gain.

3.9.2. Auto MATLAB Tuning

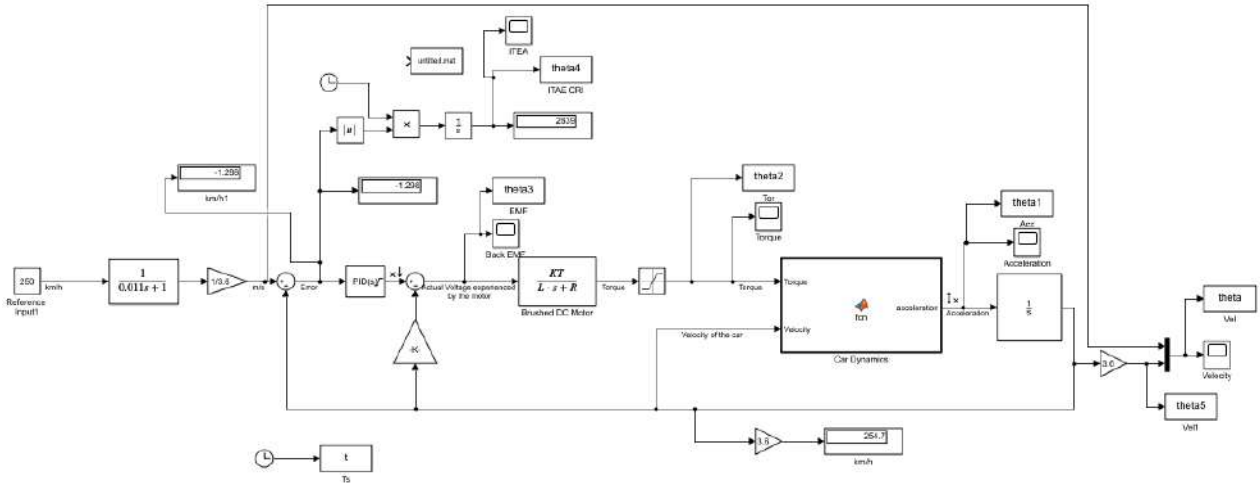

Figure 36 - Speed Control System with Linear Analysis Point added at PID and car dynamics' output

To thoroughly analyse and obtain the best response from the 'Auto-Tune' function available in MATLAB Simulink, a 'Linear Analysis Point' was added to the outcoming signal of the PID controller and one to the output of the 'Car Dynamics' block. This allowed to linearize the model through MATLAB. The results obtained were analyzed in section '*4.5.2. Auto MATLAB Tuning'*.

3.9.2.1. Using 'Interactive' Tuner Ribbon

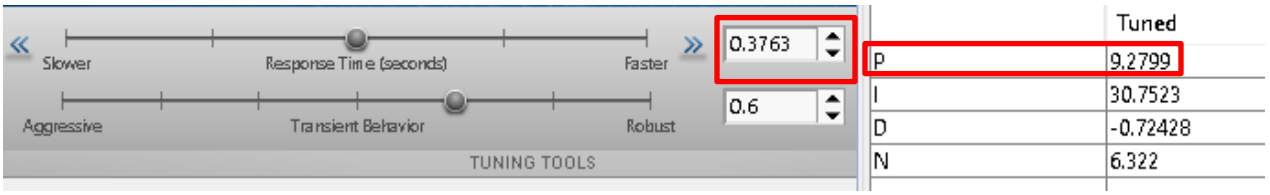

Figure 37 - Interactive Ribbon in MATLAB

Interactive ribbon shown in Figure 37 was used to slightly alter the step response generated by the auto-tuned MATLAB function. The result obtained is shown in section *'4.5.2. Auto MATLAB Tuning'*.

4. Results & Analysis / Discussion

4.1. Trial & Error Method – Overall Efficiency of the Car

'Trial and error' approach was used to determine the overall efficiency of the Tesla S P 85. This was done by varying the efficiency to obtain a speed of 100 km/h within 4.4 seconds. Equation 3.5.1. shown in section '*3.5. Modelling Car Dynamics'* was used in conjunction with the closed loop system ('*3.8. Closed Loop Response'*). The efficiency used to model the '*Car Dynamics'* block was varied to obtain these results.

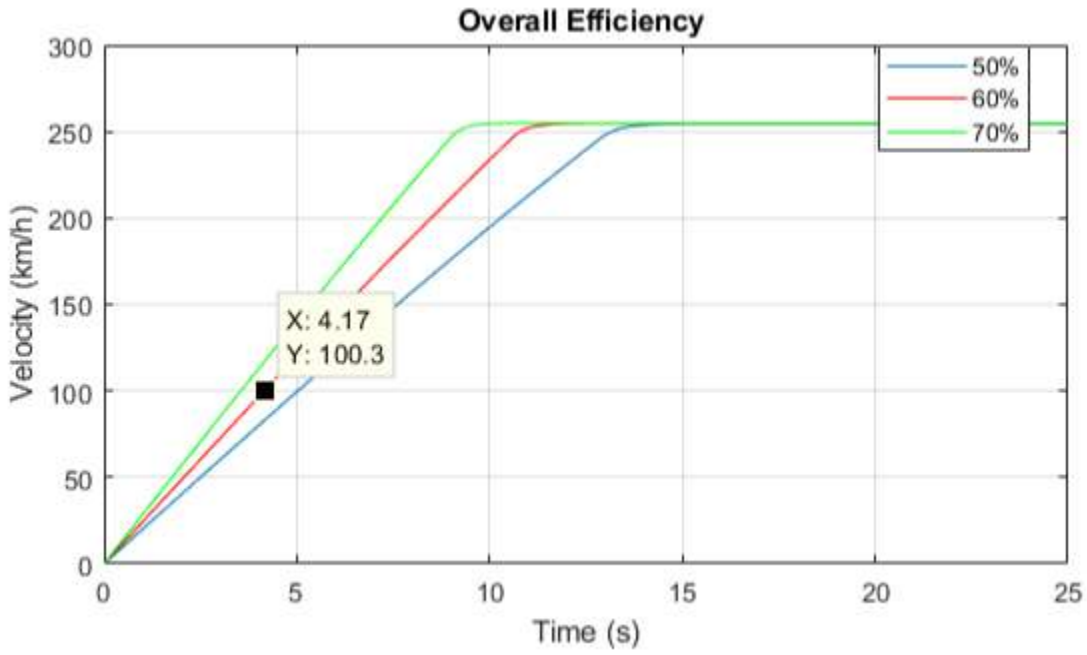

Figure 38 - Overall efficiency of the closed loop Simulink Model

Figure 38 compares the output of the closed-loop model which is the speed of the vehicle. The overall efficiency of the car dynamics was varied and applied to equation 3.5.1 to obtain the graph shown. The Simulink model was able to reach a speed of 100 km/h in 4.17 seconds at an efficiency of 60%. Although, as stated in the *'Literature Review section'* that the Tesla S P85 reaches 100 km/ within 4.2 - 4.4 seconds which is dependent on the surface and the outside environment.

Reaching 100 km/h in 4.17 was being quite reasonable considering the assumptions made and many losses ignored while constructing the Simulink model. Implementing equation 3.5.1. allowed to make up for the losses ignored. The overall efficiency of the vehicle takes into

account, the ‘slip’ of the wheels, energy wasted in the form of heat and extra drag losses etc. that were all not considered in the transfer function to model the system.

Furthermore, as the vehicle begins to accelerate, the majority of its weight is transferred to the rear back thus compressing the rear wheels while the front wheel is fully extended. The overall efficiency has allowed to compensate for all of these minute details that were not considered in the Simulink model.

Moreover, realistic bumps on the surface and the interaction of the car with various extreme conditions could also affect the speed and the efficiency of the vehicle in real life scenario which was also ignored during the modelling process.

Using the ‘Trial and Error’ method allowed to reach an efficiency that enabled the model to best replicate the actual Tesla vehicle. This model was processed further to obtain results of various control systems.

4.2. No Limitation on Battery (Current)

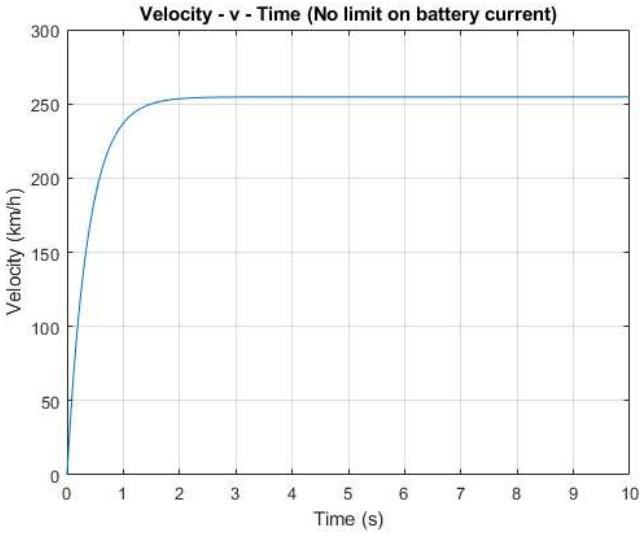

Figure 40 - Velocity - v- Time @346 input voltage (Max V = 254)

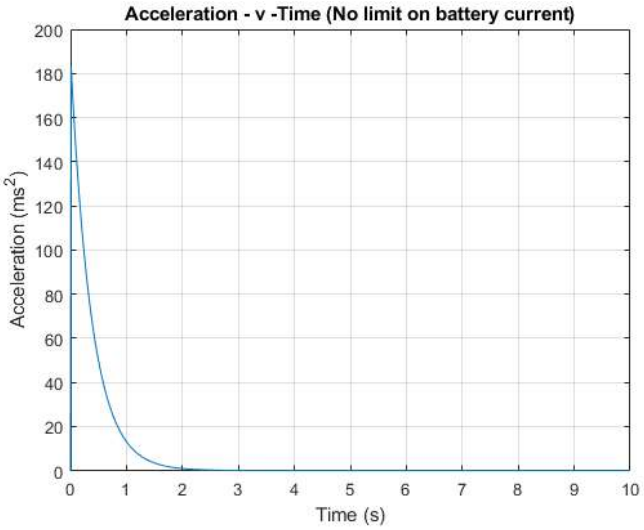

Figure 39 - Acceleration - v – Time @346V input

The Simulink model shown in section '*3.6. No Limitation'* was used to obtain these results. Figure 40 shows the velocity diagram of the model while Figure 39 refers to the acceleration one. The Simulink was able to reach its maximum velocity within 2 seconds with an acceleration of more than 180 m/s^2. This was because the model was trying to reach the final velocity as quickly as possible by withdrawing as much current possible from the battery. With no limit on the battery, the model extracted as much current possible from the battery, which would, in reality, result in 'slip' between the tyres and the surface causing the wheels to rotate without making the vehicle to move forward eventually lifting the car upwards from the surface. Due to no limit on the extraction of the current from the battery, the acceleration is too great, higher than those of fighter jets. Hence, classified unrealistic.

Figure 41 shows the torque produced by the motor through extracting current from the battery. The graph shows a maximum torque of 16, 000 Nm while the maximum of Tesla S P85 derived from the literature review and shown in section '*3.3. System parameters'* was 600 Nm. A torque of 16, 000 was inconceivably more compared to the actual torque of the Tesla vehicle. It was apparent from observing the graph that the model was trying to reach the input voltage (speed) as swiftly as possible, and once speed was achieved, a drastic decrease in torque and acceleration was detected. The minimum torque reached was 86.63 Nm which illustrated the requirement to maintain the velocity of 250ms. In other words, the motor needs to provide a constant torque of 86.63 Nm to maintain the velocity of 250ms. However, that is not the torque needed to reach the velocity of 250ms.

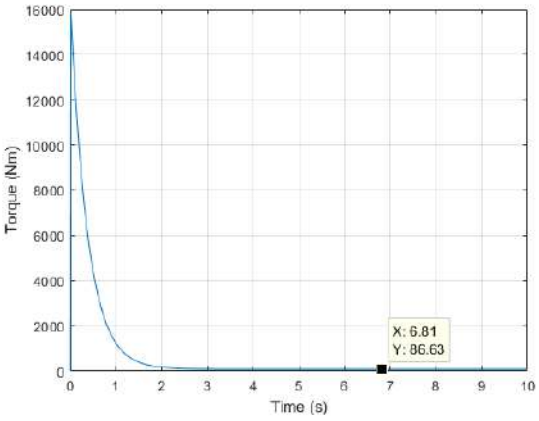

Figure 41 - Torque - v - Time @346V input

4.2.1. Applying Flemings Right Hand & Lenz law

$$FRHR \qquad E_b = \frac{NP\phi Z}{60A} \qquad eqn.\ 4.2.1.1.$$

Equation 4.2.1.1. shows the Flemings Right Hand Rule (FRHR) in a mathematical form, where;E_b is the induced EMF or the back EMF of the DC motor, N is the speed and ϕ is the flux.

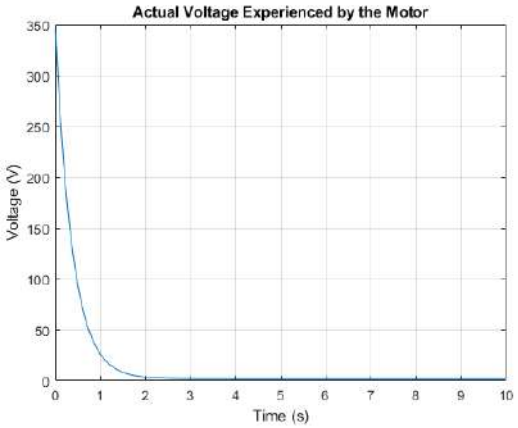

Figure 42 – Used to analyze back EMF @346 input voltage

Applying Flemings Right Hand Rule to the modified DC motor resulted that *'the direction of the induces emf is opposite to the applied voltage'* (Circuit Globe , n.d.).

Lenz's Law $$E_b = -N\frac{\Delta\phi}{\Delta t}$$ *eqn.* 4.2.1.2.

Lenz's law, one of the essential laws governing the DC motor operation states that '*the polarity of the induced EMF is such that it produces a current whose magnetic field opposes the change which produces it'* (COLLINS, n.d.). Implementing this statement to the model would simplify Lenz's law to:

$$Net\ voltage\ across\ the\ motor = supply\ (initial) voltage + (\pm back\ EMF) \quad eqn.\ 4.2.1.3.$$

Now considering the equation mentioned above to analyse the back EMF graph shown in Figure 42, the initial peak in the voltage to 346V was because initially, the motor was not rotating, resulting in zero back EMF thus, maximum torque. However, as the motor began to rotate, it started to produce back EMF and eventually became equal to the initial voltage of 346V. The outcome of this was almost zero voltage but would never reach a figure of zero because the car would need to compensate for the aerodynamic drag and rolling resistance as deduced by the mathematical model in *'section 3.1.'*.

4.2.2. Limiting the battery performance

It was not only important to replicate the motor of the Simulink model to the actual Tesla S P85 model but also to ensure that important limitations were applied to relevant components i.e. battery to make it more realistic.

One of the ways to tackle this was to limit the current, the motor can withdraw from the battery through the use of 'Saturation' block in the MATLAB Simulink. Saturating the output of the motor limited the torque produced hence, limiting the current. This was because current is directly proportional to the torque generated by the motor as explained in section '*2.0 Literature review'*. This would be analysed in-depth in the next section; open loop analysis.

Having no limitation on the battery had allowed to analyse the core fundamentals of the Simulink Model and to understand the impact of back EMF. Now, it would be much simpler to analyse the control system.

4.3. Open Loop Model Analysis

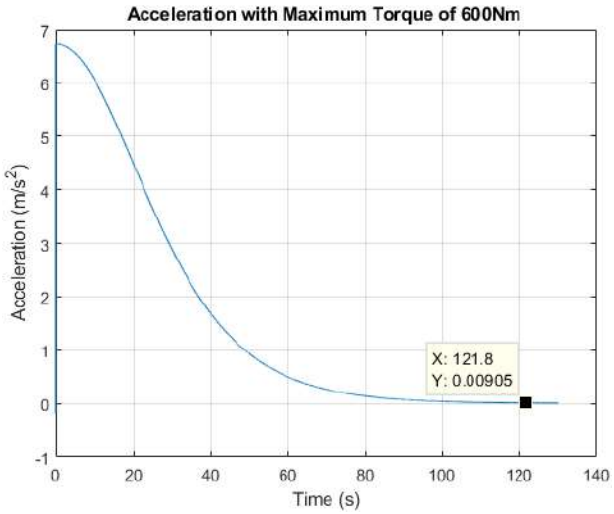

Figure 44 - Acceleration of the open loop model with torque caped

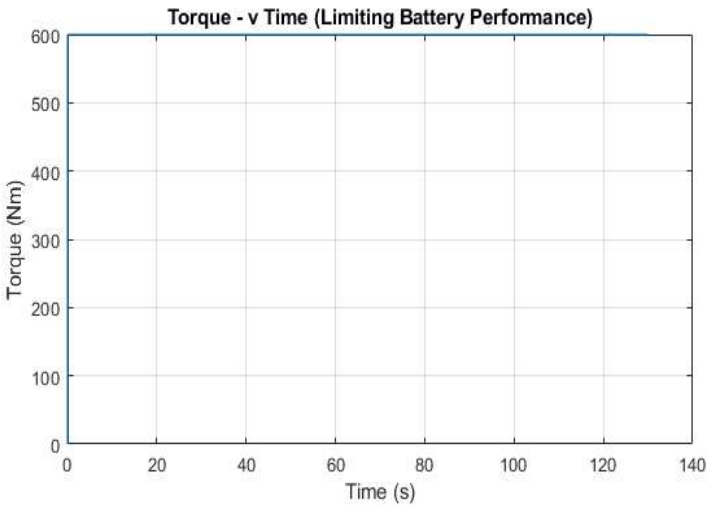

Figure 43 - Torque of the Open loop model

A 'Saturation' block function was implemented after the DC motor block in the Simulink to cap/limit the torque produced by the motor to 600 Nm; the maximum torque a Tesla S P85 can generate. This impacted the acceleration of the vehicle but more importantly massively affected the torque produced by the motor, making it more realistic to the practical world. The 'Saturation' block used is shown in Figure 45. It was also possible to directly saturate the current supplied by the battery however, it would require making two separate transfer functions; one for limiting the current and the other that produces torque with respect to the current as an input. Though, it would result in the same outcome but would make the Simulink model much more complicated.

Comparing Figure 44 with Figure 39 both depicting the acceleration but one had a limit on torque while the other did not. The profile of both graphs was pretty much the same except that Figure 39 had a steeper slope than in Figure 44. However, after limiting the torque (Figure 44), the acceleration value had drastically reduced since the motor can only withdraw a limited amount of current from the battery source. An acceleration of more than 180m/s^2 was reduced to 6.8m/s^2 hence, making it much more realistic.

Figure 43 made it much more transparent, the effect of capping the battery performance. The torque of 600Nm was produced and stayed constant throughout since it was an open loop model with no feedback loop. The

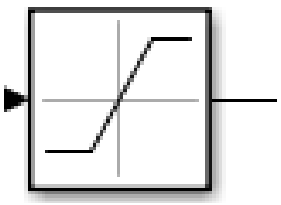

Figure 45 - Saturation Block

output not being fed back to the input positively impacted the torque. The open loop model helped to limit battery performance. Having specified and implemented the limitations, now it would be worth analysing the closed loop model.

The velocity of the open loop model is shown in Figure 46 with a maximum velocity of over 700ms. This was due to no feedback loop, but most importantly by observing the open loop model shown in section *'3.7. Open Loop Response'* and comparing it with Figure 25, the effect of back EMF and gear ratio was apparent. With no feedback loop, the model attempted to reach a maximum velocity that it can, but it was limited to 734 km/h due to the cap on the battery performance limiting the torque produced.

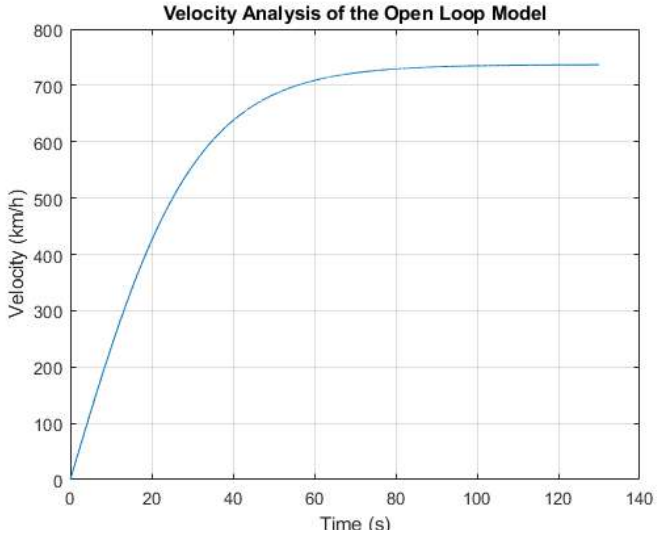

Figure 46 - Velocity of the Open loop model

4.4 Closed Loop Model Analysis

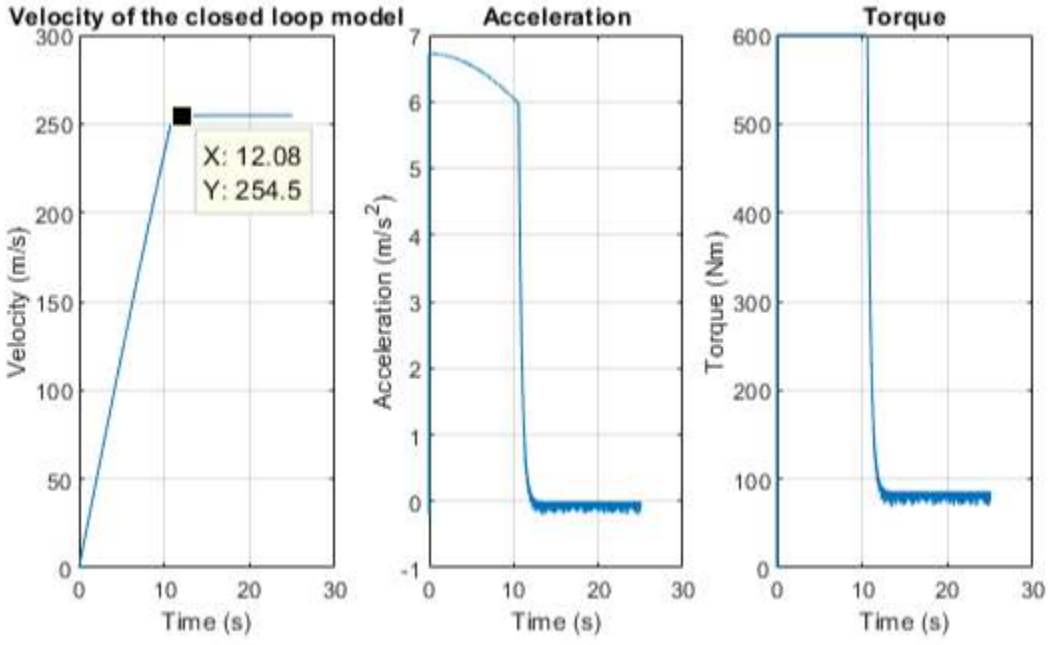

Figure 47 - Velocity, Acceleration and Torque of the Closed Loop Model shown in section '3.8. Closed Loop Response'

Figure 47 shows the velocity, acceleration and torque with respect to time of the closed-loop model. The model was able to reach its maximum velocity within 12 seconds with a reference input voltage of 346V. The velocity consistently increased with a linear gradient till 12 seconds after which it stayed constant throughout the runtime. This was because the vehicle was accelerating during the initial 12 seconds period with a maximum torque that the motor can produce.

Figure 47, the acceleration raised intensely during the first second and then started to gradually decrease non- linearly until 10 seconds. This was due to the drag force increasing progressively with the velocity. However, after 10 seconds, the acceleration and the torque dropped drastically which was due to the increase in the back EMF. Furthermore, the acceleration went to zero once the maximum speed of 254m/s was achieved but the torque remained constant at 80 Nm. This is the amount of torque that needs to be produced by the motor for the vehicle to maintain the speed of 254m/s.

4.5. Control System Analysis

4.5.1. Manual/Heuristic Fine-Tuning (Zeigler Nichols)

P Controller (Proportional Gain)

It was deduced in section *'3.9.1.'* that the P-proportional gain was greater than 23.5 ($K_p > 23.5$). Therefore, '*Trial and Error'* method was used to determine the suitable value that best suited the system parameters/conditions set in sethe ction '*3.3'*. It should be noted that other gains were set to zero.

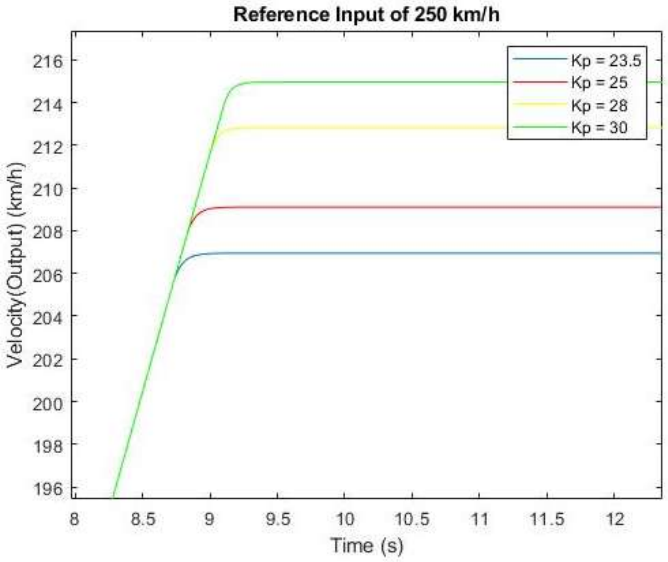

Figure 48 - Various P-proportional gain are compared with a reference input of 250 km/h

Figure 48 compares different proportional gain by using trial and error method slightly influenced by the Zeigler Nichols Design Method which was explained in the '*Literature Review'*. Zeigler method was used to deduce the minimum tuning value of proportional gain.

Figure 48 shows that all four Kp values; 23.5, 25, 28 and 30 meet the specified 'Rise Time' of 15 seconds. All four proportional gains considered did meet the performance criteria set but failed to reach the reference input value/speed. Hence, it was worth analysing higher values as well which was done later in this section. From '*Literature Review'* section, implementing I-integral gain not only allowed to meet the reference input but also increased the overshoot, keeping this in mind it was reasonable to select Kp of 25 since introducing I-integral would allow the controller to respond faster.

Though the proportional gains shown in Figure 48 were well within the 'Rise Time' limit and other parameters, one of the major issues was that the controller failed to reach the specified 'Reference Input'. It was possible to consider higher Kp values to achieve the desired input value by only using Proportional gain but may seem unrealistic. The result obtained is shown in the graph below.

Just to check the effect of taking proportional gain as 1, 000, a graph was plotted in Figure 49 which suggested that the control system was almost able to reach the 'Reference Input' value of 250 km/h. Though any further increase in the proportional gain would not affect the outcome due to the steady-state error as explained in *'Literature Review'*.

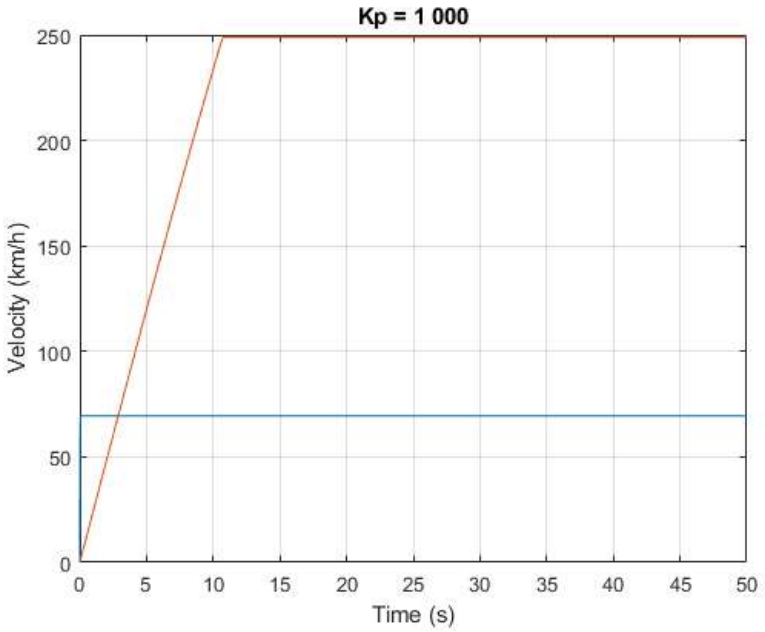

Figure 49 - Proportional gain of 1, 000

The control system with a proportional gain of 1, 000 did not make the velocity to oscillate which should happen as the proportional gain increases as proven in the journal written by (Li, 2006)

and stated in the '*Literature Review'* section. This was due to the 'Saturation' block used to limit the torque produced by the motor by capping the current displaced by the battery. In other words, 'Saturation' block provides an additional layer of stability to the control system and compensate for any extreme controller outcome.

Increasing the P-proportional gain, K_p led to the reduction of rise time and the steady-state error however, due to power and actuator limitations, the P-proportional gain could only be increased to a certain extent since changing the speed of the vehicle from 0 to 10 m/s within 0.4 or less seconds is not possible in the real speed control systems. (Carnegie Mellon University , n.d.).

Hence, P-controller did not suffice the system parameters; thus, the need to use I-integral gain in order for the output to reach the reference value.

PI Controller (Integral Gain)

Adding integral gain to the proportional gain allowed the output to each the 'Reference Input' value. An integral gain of 8 was added to the proportional gain of 25 to transform the control system into a PI controller.

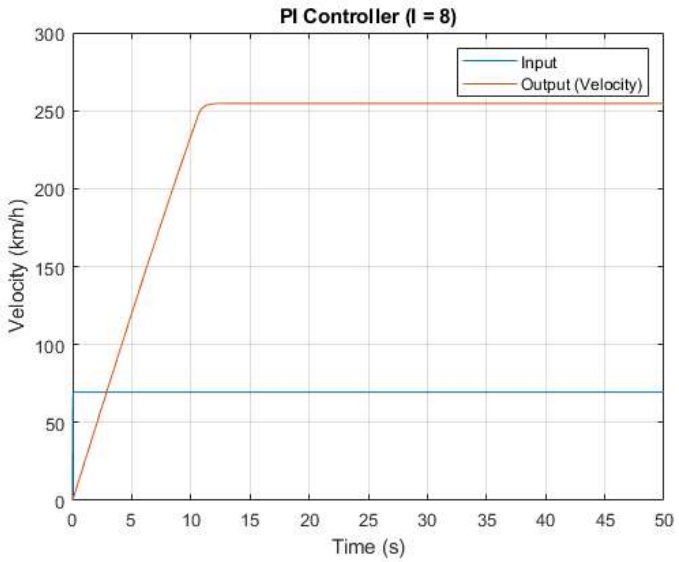

Figure 50 - PI Controller (P = 10, I = 5). Maximum velocity reached = 254 km/h

Figure 50 shows the impact, the integral gain made on the outcome. Now, the controller was able to produce the desired value. However, the PI controller went over the required outcome by 4 km/h due to the steady-state error which was more than 1% of 250 km/h. Hence, the PI controller did not meet the steady-state error parameter of 1%. Although, it did satisfy all the other specified parameters stated in *'Section 3.3.'*. Therefore, introducing D-derivative gain may allow the system to become more sensitive and would also make the transition period much smoother.

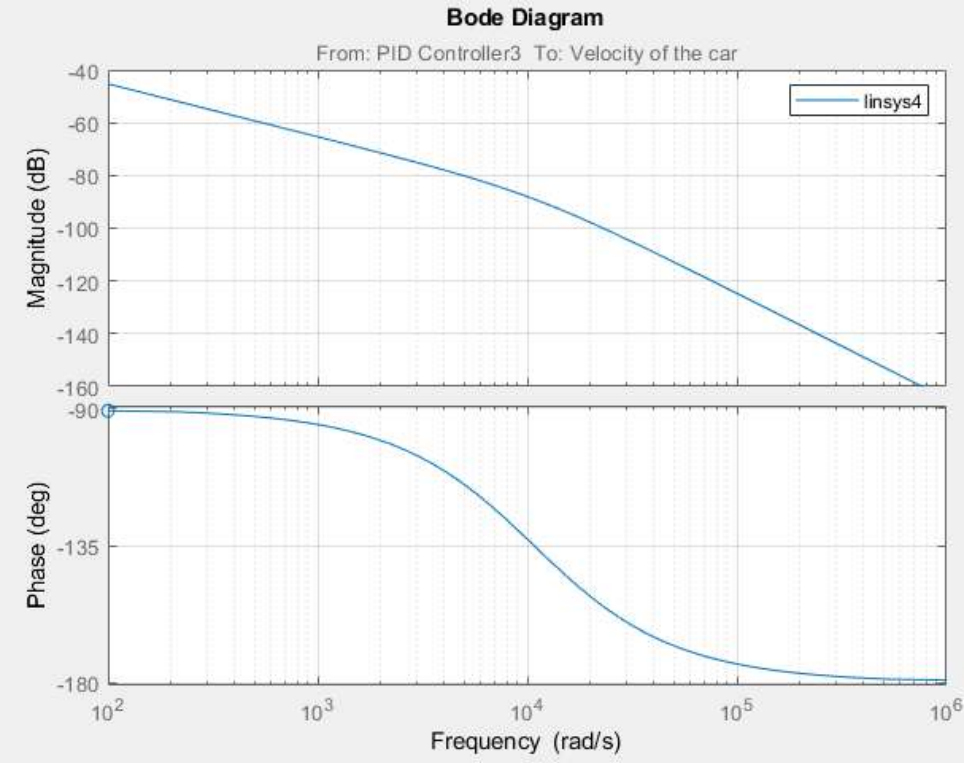

Figure 51 - Bode Diagram of the PI controller

Bode diagram is plotted and shown in Figure 51 to evaluate the loop stability margin. By observing the plot, it was evident that it was a second-order function with two single poles that did not cross the zero-decibel line and the phase angle never reached -90 or -180 degrees. Hence the gain and the phase margin equivalate to infinity which suggested that the system was stable however, would perform poorly, struggle to eliminate the steady-state error.

PID Controller (Derivative Gain)

Derivative gain of 8 was applied in conjunction with the 'Anti-Wind Up Clamping' block function to reduce the steady-state error. This function was extracted from the journal written by (Liu, 2017). The impact of this function on the Simulink model was explained in the *'2.8.1. Literature Review'* section.

Implementing the 'Anti Windup Clamping' function allowed to reduce the steady-state error of the control system as it disabled the I-integral gains to wind up.

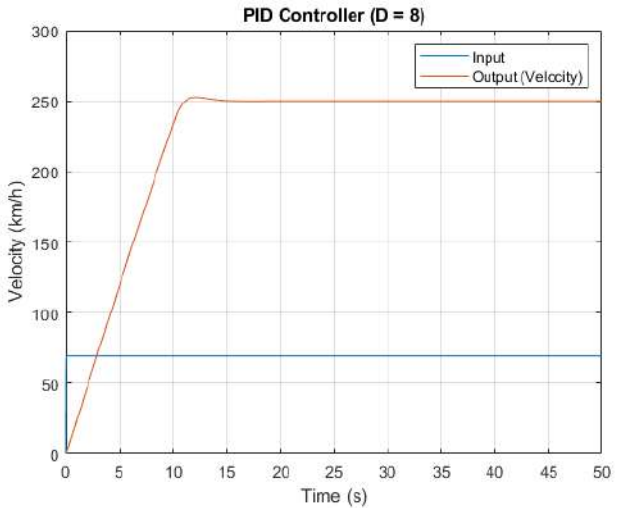

Figure 52 - PID Controller (D = 8); Maximum velocity = 252 km/h

Implementing derivative gained allowed a smooth transition between the overshoot and the reference speed of 250 km/h in this case. This had undoubtedly increased the settling time; however; it was still below 15 seconds which was the maximum limit set as a criterion for the controller. The effect of adding a slightly higher D-derivative gain resulted in a smoother transition would be apparent in the comparison against the 'Auto Tuned' response.

In summary the manually tuned PID controller had the following parameters:

P-proportional gain = 25

I-integral gain = 8

D-derivative gain = 8

4.5.2. Auto MATLAB Tuning

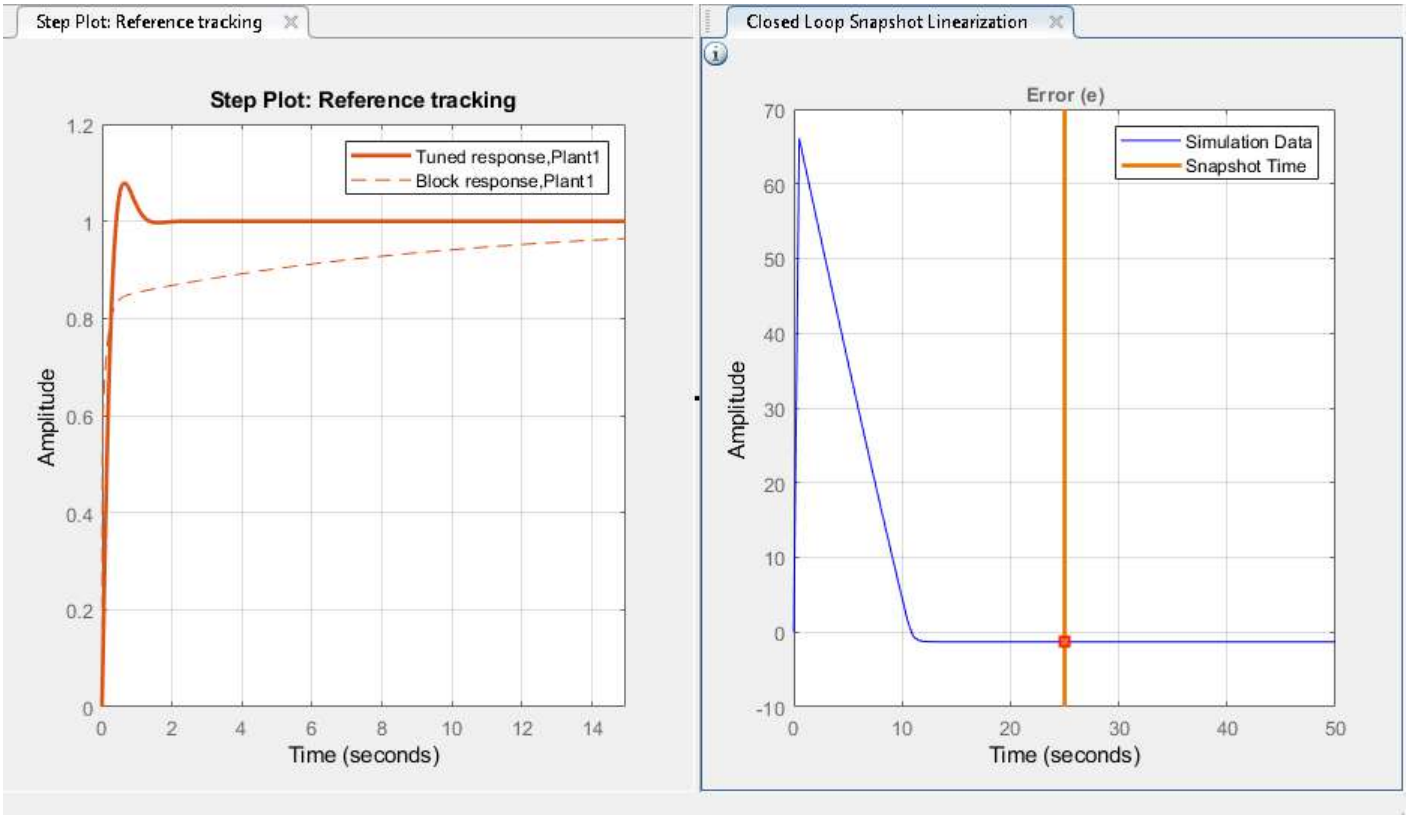

Figure 53 - Compares the 'Step Response' of the Manual and the Auto tuned control system

NOTE: The solid orange line represents the system which was tuned through MATLAB function while the dotted line represents the system response of the manually tuned PID control system

The manually tuned PID control system with proportional, integral and derivative gains of 25, 8 and 8 respectively was processed through the 'Auto-Tune' function of the MATLAB. The 'Step response' and the 'Linearization graph' are shown in Figure 53.

Notice that the auto-tuned response had an overshoot and not so smoother transition while the manually one did not. However, the manually tuned PID had a higher settling time and took thrice the time of the auto-tuned response. This is discussed later on when using the 'Interactive Ribbon' function.

The closed-loop auto-tuned PID control system was linearised using the 'Re-Linearization' function and is also shown in Figure 53. It suggested a linear increase in the error as the system reached its peak speed then, a linear decrease to overcome the overshoot before reaching a steady value to -1.3, indicating a steady-state error in the system.

Figure 54 compares the disturbance rejection of the manual and the auto-tuned response that measured the ability of the control system to overcome the effects of disturbances. In other words, as stated in the '*Literature Review'* while analysing the article written by (National Instruments , n.d.), '*defines the worst case conditions in which the control system is expected to meet design requirements'.*

The auto-tuned response had a better disturbance rejection compared to manual at an input reference of 250 km/h.

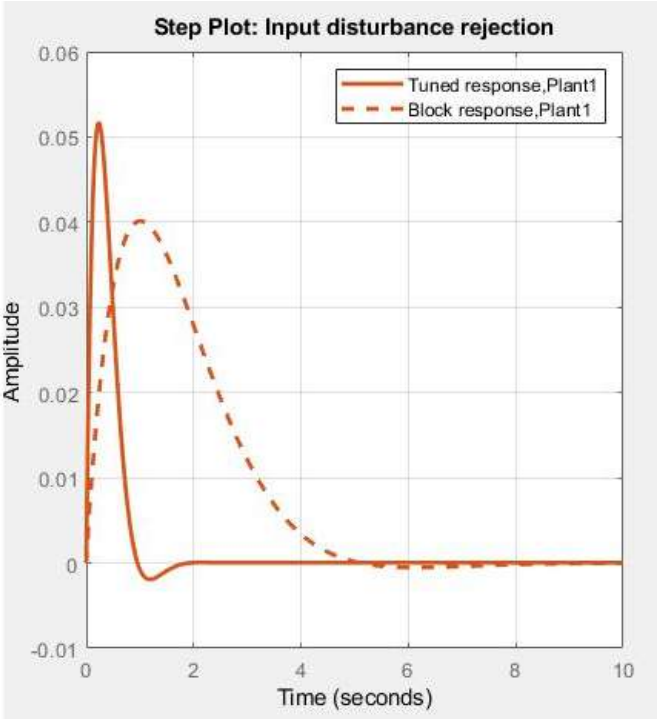

Figure 54 - Comparison of Disturbance Rejection between the manual and MATLAB auto tune.

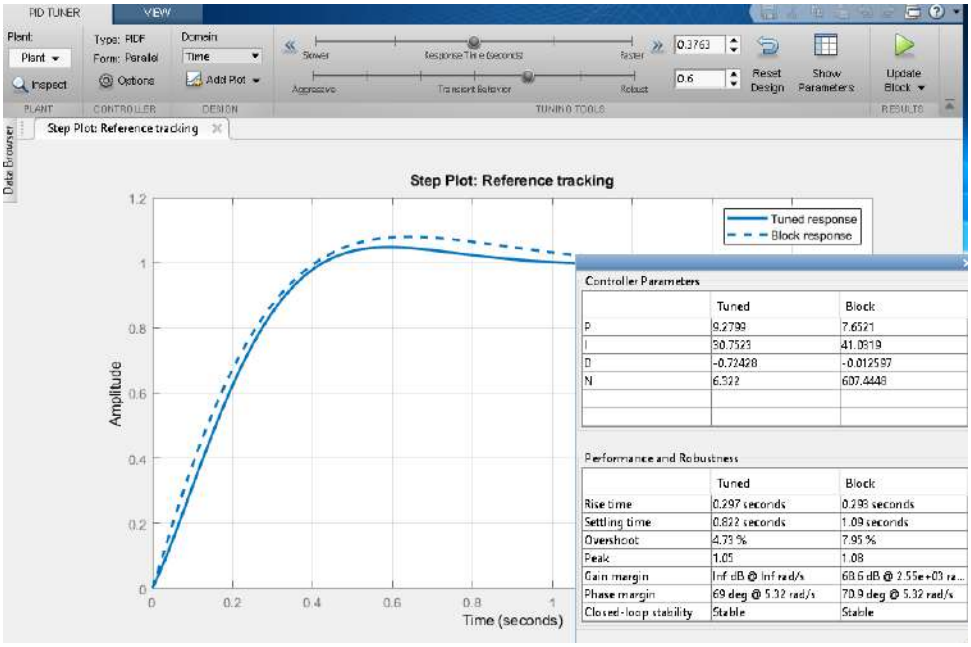

Figure 55 - Interactive Ribbon used to reduce the overshoot

The blue dotted line shows the auto-tuned response while the sold blue line represents the response of the controller which was altered using the interactive MATLAB ribbon shown in section *'3.9.1.'*. The interactive ribbon was used to slightly reduce the overshoot approximately by 3% as well as the settling time as shown in Figure 55.

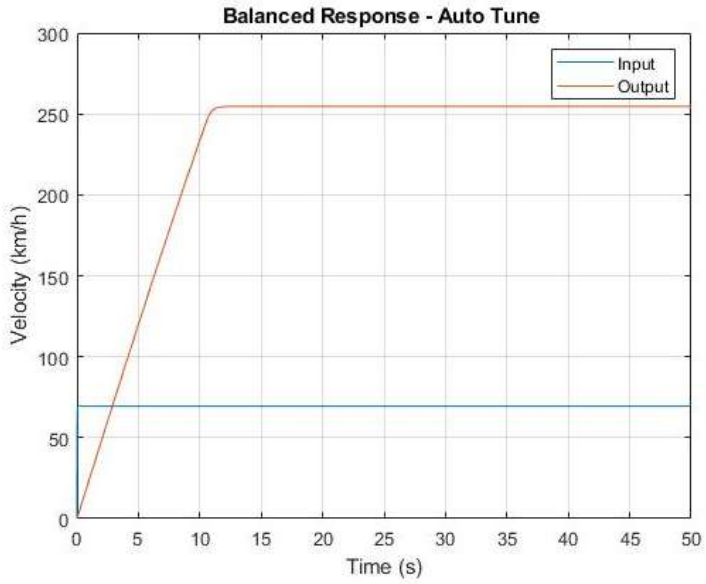

Figure 56 - Output velocity of the system auto tuned system

Figure 56 shows the output velocity of the auto-tuned PID controller, altered through 'Interactive ribbon'. The rise time and the settling time was all within the criteria set however, it failed to reach the reference input due to steady-state error. Although, the auto-tune function used the integral gain of 30 but still the system failed to reach the reference input. This could be due to the amendment in the 'Filter Coefficient (N) shown in Figure 55 however, the impact it had was not analysed in this report. Hence, the manually tuned PID performs significantly better with a steady-state error of zero.

4.5.3. Comparison of manually tuned (P, PI & PID) and auto tuned PID control system

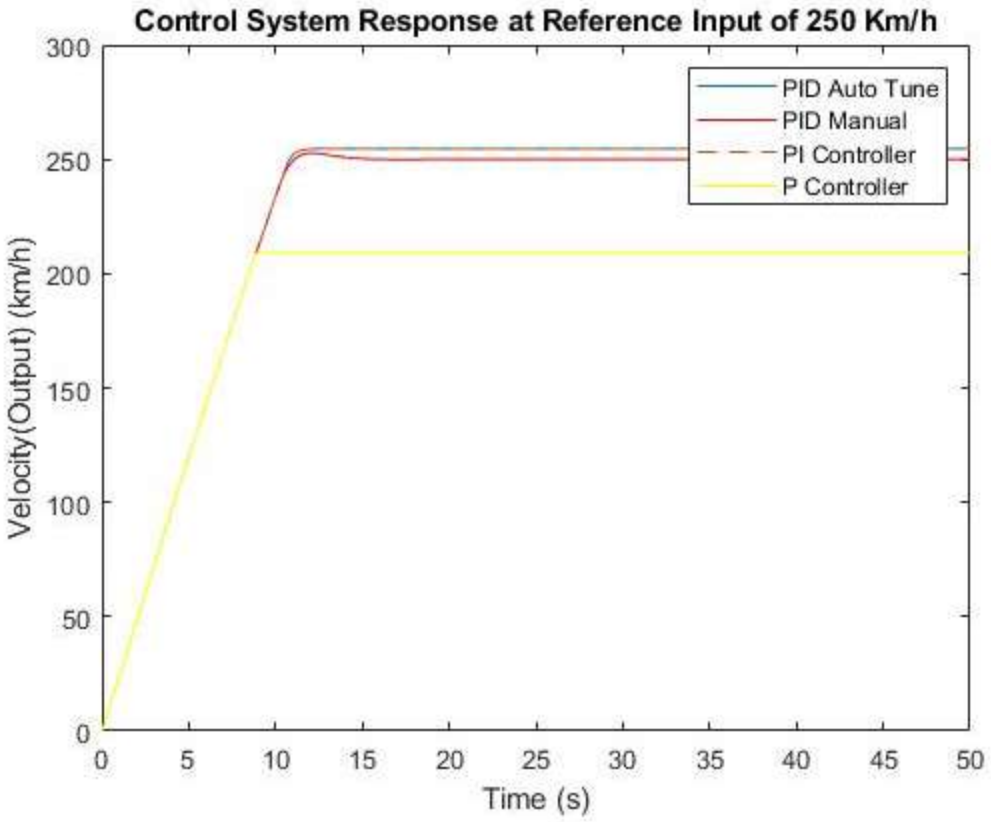

Figure 57 - Comparison of tuned controllers

	Manually inspired by Zeigler Nichols			MATLAB Autotune
Controller Parameter	**P Controller**	**PI Controller**	**PID Controller**	**PID Controller**
P	25	25	25	9
I	0	8	8	30
D	0	0	8	-0.7
Performance & Robustness				
Rise Time (sec)	9.2	11.5	10.7	12
Settling Time (sec)	9.2	11.5	14.8	12
Overshoot (km/h)	Way under	4.7	2.7 (1.06%)	4.7
Peak (km/h)	209	254.7 (1.8%)	252.7 (1.06) %	254.7
Closed Loop Stability	Yes	Yes	Yes	Yes
Steady State Error	Yes	2%	No	2%

Table 1 - Comparison of tuned controllers at 250 km/h

NOTE: Filter coefficient (N) was not compared

NOTE: The P controller with Kp of 1, 000 was not considered as it was impractical

By observing the performance of tuned controllers shown in Table 1, it was apparent that manually tuned PID outperform the rest in most of the parameters except the 'Settling Time'. The primary issue with PI controller and the auto-tuned PID controller was the steady-state error of1.82% which had significantly affected their performance since 1% was the performance specified in section 3.1. Hence, manually tuned PID was opted as the better option while PI as the next best alternative.

5. Evaluation

It was essential to revisit and examine the aims and objectives set at the beginning of this report in order to assess the implementation of the speed control system on Tesla S P85. This report intended to design an electric car model based on Tesla S P85 through mathematically scrutinising the relevant components of the vehicle and processed it further to model speed control system using MATLAB Simulink. Moreover, various controllers were considered to regulate the speed and the response was compared against set performance criteria. Seven objectives were set which were shown in section *'1.2. Aims and Objectives'* and are as follows:

5.1. Examine the vehicle dynamics of Tesla S P85 model from an engineering perspective

The dynamics of Tesla S P85 model was examined in section *'2.4. Tesla S P85 Vehicle Dynamics'* that formed a part of the literature review. Main components which profoundly impacted the model i.e. input, battery, motor and wheels were assessed from an engineering perspective. Moreover, a thorough analysis was done during which other essential factors such as aerodynamic drag or the limitation imposed on the model by battery performance were considered.

The efficiency of the three-phase and four-pole AC induction motor was also considered in respect to the motor speed and motor torque. After in-depth analysis, it was concluded that brushed DC motor with specified parameters was able to replicate Tesla AC induction motor when implemented in the Simulink model. The DC motor that mimicked the performance of the Tesla AC induction motor was summarised in equation 3.1.2.12. which was used immensely to construct the brush DC motor in MATLAB Simulink.

5.2. Derive and develop mathematical model behind the vehicle dynamics

Once in-depth examination on Tesla S P85 model was completed, it was essential to process the information obtained in the '*Literature Review'* section with regards to the vehicle dynamics to derive and develop a mathematical model. The derived mathematical model was shown in section '3.1. Mathematical Model / Vehicle Dynamics' which was separated into seven sections each considering a different aspect of the mathematical model. Engineering laws; Newton's second law, Ohms law, Kirchhoff's law etc. were all taken into consideration and were implemented

successfully during the development process of the mathematical model. Equation 3.1.7.1 summarised the vehicle dynamics which was transformed into MATLAB Simulink to design the dynamics of the car as shown in section *'3.4.2 Mathematical Model'*.

Moreover, the internal structure of Tesla's battery was extracted from the '*Literature Review'* specifying the electrical properties which were derived to model the battery. Furthermore, assumptions were made during the modelling process such as the reduction of the wheel radius due to compression under weight to ensure that the model was kept within the scope of the project while also not making it unreasonable complex or unrealistic. However, they are pointed out and made clear.

5.3. Determine the forces acting on the vehicle as it moves

Forces acting on the vehicle significantly impacted the performance of the model. The control system was determined and analysed during the development of the mathematical model in section '*3.1. Mathematical Model'*. Major contributing forces including; aerodynamic drag, traction force, rolling resistance, motor traction etc. were all deduced through relevant equations and method including Newton's second law (F = ma) to obtain values and equations which then be transformed into MATLAB Simulink. These forces were also used to obtain the efficiency of the vehicle as it significantly impacted the efficiency curve of the modelled system.

5.4. Implement engineering model in MATLAB Simulink

In order to implement the designed mathematical model into MATLAB Simulink, it was necessary to use main functional blocks and transfer functions available in MATLAB library. The brushed DC motor with modified parameters, vehicle dynamics and the battery were all implemented in MATLAB Simulink as shown in section '*3.4. Modelling Brushed DC Motor', '3.5. Modeling Car Dynamics'* and *'3.6. No Limitation on Battery'* respectively. A Simulink model with no limitation on the battery was first considered to analyse and understand the core fundamentals of the Simulink model including the impact of the back EMF.

5.5. Identify and evaluate relevant techniques to design control systems to regulate the speed of Tesla model.

Appropriate techniques to regulate the speed of the control system were identified and evaluated in *'Literature Review'* section as well as assessed from a mathematical perspective in the section *'3.2. Mathematical Model of PID controller'.* Relevant techniques involved the use of P, PI, PID controllers with appropriate gains.

5.6. Implement, test and tune the control system that correlates to the requirement to regulate the system.

Once the MATLAB Simulink was constructed representing the Tesla S P85 with the controllers applied, various methods were implemented to tune the controllers' response in accordance to the performance criteria set in section *'3.3 System Parameters'*. Tuning methods included manually tuning which was slightly inspired by the Ziegler Nichols method and the auto-tuning method. The control system with the controller implemented is shown in section *'3.8. Closed loop response'* which was used to test and obtain results shown in section *'4.5. Control System Analysis'*. The testing also involved evaluating the velocity, acceleration diagram as well as the Bode diagram which allowed to test the stability of the control system. Linear analysis was also performed on the auto-tuned control system, allowing indicate the steady-state error.

5.7. Compare the performance of each modelled control systems

The data gathered of different controllers were compared as shown in section *'4.5.3.'* to deduce the best option with respect to the performance criteria set. The comparison was done between manually tuned P, PI and PID and the auto-tuned PID controller. It was apparent from Table 1 that manually tuned PID performed the best under the applied conditions. The only major drawback of auto-tuned PID was the steady state error but otherwise performed equally good.

In summary, it was apparent from the evaluation of the report that all the original objectives set in the first section of the report were met decisively though there is still space for further work.

6. Conclusion

In conclusion, it was understandably complex to model a speed control system replicating Tesla S P85 since only limited good sourced information was available as the manufacturer does not consider 'Corporate Social Responsibility' as an important factor. Hence, analysing the Tesla AC induction motor to replicate it using a brushed DC motor required accurate and precise interpolation of the limited data available while also implementing 'Trial and Error' method to determine the efficiency of the vehicle.

The aim goal of the report was to model the Tesla S P85 and implement a control system regulating the speed. The first section of the report laid out the objectives and the scope of the project which pointed out the limitations and the context in which it was being carried out. The second section, '*Literature Review'* dealt with researching and gathering relevant well-sourced data which was derived throughout the report particularly to model the system mathematically. The mathematical model was then transformed into the MATLAB Simulink depicting the control system with various controllers. The results obtained from the Simulink were used to evaluate each controller as well as the tuning method to come up with the best-analysed option.

The mathematical model allowed to determine major limitations of the vehicle and to derive important parameters of the system. The transfer function representing brushed DC motor, $T(s) = 0.25 * \frac{V(s) - 0.12 * \omega(s)}{(493 * 10^{-9}s) + (5.3 * 10^{-3})}$ mimicked the response of the Tesla AC induction motor while the equation, $\frac{0.6 * 40.5T - 413 - 0.3381v^2}{2108} = \frac{dv}{dt}$ portrayed vehicle's dynamic.

Furthermore, the open and closed loop Simulink model depicting the performance of S P85 ensured a successful transformation of the mathematical model into the MATLAB Simulink. The results obtained very much replicated the real-life performance of the vehicle considering the fact that assumptions were made throughout the building process.

Moreover, Tesla Simulink model was process further by implementing a control system and applying various controllers to regulate the speed. The P controller was not able to reach the reference input while the PI controller manually tuned and the PID controller auto-tuned both had the same steady state-error issue. Many attempts were made to resolve this issue i.e. considering

the ‘PI compensator’ but the issue persisted. Though the results of those attempts are not shown in this report due to limited space.

Lastly, a comparison between various controllers and tuning methods were drawn to select the best available option. The manually tuned PID controller best suited the specified performance criteria as the overshoot was well below 10% (1.06%), rise time below 15 seconds (10.7), settling time of just under 15 seconds (14.8) while it was also stable and had a steady-state error of zero. Thus, it best satisfies all the performance criteria set.

Overall, considering the goals and objectives of the project, it was concluded that the report successfully met all the set requirements.

6.1. Recommendations & Further work

The recommendation would be to consider the ITAE analysis which would allow to evaluate the response with respect to time. The control system shown in Figure 31 consists of ITAE criteria; however, the results obtained are not shown nor analysed due to limited space.

While for further work, it would be worth implementing Fuzzy logic to evaluate the impact of the surface inclination on the control system. Additionally, implementing autonomous emergency braking would make the system much safer for the end users.

Word Count: 12, 360

7. Bibliography

University of Cambridge. (n.d.). *Newton's Second Law*. Retrieved from Issac Physics : https://isaacphysics.org/concepts/cp_newtonii

ARTICLES, T. (n.d.). *Tesla Polyphase Induction Motors*. Retrieved from Allaboutcircuits.com: https://www.allaboutcircuits.com/textbook/alternating-current/chpt-13/tesla-polyphase-induction-motors/

Astrom, K. J. (2002). PID Control . *Control System Design* .

ATO. (2019). *3 hp (2.2kW) 3 phase 4 pole AC Induction Motor*. Retrieved from ATO.com: https://www.ato.com/3-hp-2-2kw-3-phase-4-pole-ac-induction-motor

B, J. (n.d.). *Tesla Model S P85 specs*. Retrieved from Fastestlaps: https://fastestlaps.com/models/tesla-model-s-p85

Bakker, S. (n.d.). *Induction Motor Is The Ideal Choice For The 21st Century Electric Car | CleanTechnica*. Retrieved from CleanTechnica: https://cleantechnica.com/2016/05/30/nikola-teslas-19th-century-induction-motor-ideal-choice-21st-century-electric-car/

Bissell, C. (1988). *Control Engineering* . London: Van Nostrand Reinhold (International).

Bolton, W. (2002). *Control Systems.* Oxford.

Cain, T. (2014, August 25). *2013 Tesla Model S P85 Performance Review - NOT A Very Range-Limited Car On A Range-Limited Island*. Retrieved December 02, 2018, from goodcarbadcar: https://www.goodcarbadcar.net/2014/08/2013-tesla-model-s-p85-review-canada-pei-test-drive/

Carnegie Mellon University . (n.d.). *Cruise Control: PID Controller Design* . Retrieved from ctms: http://ctms.engin.umich.edu/CTMS/index.php?example=CruiseControl&section=ControlPID#1

Chen-Yu-Hsieh. (2014). Energy Harvesting and Control of a Regenerative Suspension System using Switched Model Converter . *SIMON FRASER UNIVERSITY* .

Circuit Globe . (n.d.). *Back EMF in DC Motor*. Retrieved from Circuit Globe : https://circuitglobe.com/what-is-back-emf-in-dc-motor.html

Clarke, S. (2017, December 21). *How green are electric cars?* Retrieved from The Guardian: https://www.theguardian.com/football/ng-interactive/2017/dec/25/how-green-are-electric-cars

COLLINS, D. (n.d.). *Lenz's Law and Back EMF*. Retrieved from Motion Control: https://www.motioncontroltips.com/lenzs-law/

CSE. (n.d.). Implementing PID Controllers.

CSRHUB Team . (n.d.). *Corporate Socila Responsibility (CSR) & Environmental, Social, Governance (ESG) Metrics* . Retrieved from CSRHUB: https://www.csrhub.com/CSR_and_sustainability_information/Tesla-Motors-Inc

Dudovskiy, J. (2018, October 21). *Tesla CSR: a brief overview* . Retrieved from Reseach Methodology : https://research-methodology.net/tesla-csr-a-brief-overview/

Electronics . (n.d.). *Closed-loop Systems*. Retrieved from Electronics Tutorials : https://www.electronics-tutorials.ws/systems/closed-loop-system.html

Electronicstutorials. (n.d.). *Kirchhoff's Voltage Law*. Retrieved from Eletronicstutorials: https://www.electronics-tutorials.ws/dccircuits/kirchhoffs-voltage-law.html

Engineering Corporation. (2004). *Electrical Induction Motors - Synchronous Speed*. Retrieved from engineeringtoolbox: https://www.engineeringtoolbox.com/synchronous-motor-frequency-speed-d_649.html

Engineeringtoolbox . (n.d.). *Electric Motors - Power and Torque vs. Speed*. Retrieved from Engineerintoolbox: https://www.engineeringtoolbox.com/electrical-motors-hp-torque-rpm-d_1503.html

Erik Gregersen, B. A. (2018, October 04). *Tesla, Inc.* Retrieved November 18, 2018, from Encylopaedia Britannica: https://www.britannica.com/topic/Tesla-Motors

Gershgorn, D. (2018, July 25). *Waymo just laid out its vision for a driverless future*. Retrieved from qz: https://qz.com/1336116/waymo-just-laid-out-its-vision-for-a-driverless-future/

Government, U. S. (1976). *Electric Vehicle Act 1976.* https://www.fordlibrarymuseum.gov/library/document/0055/1669499.pdf: The White House.

Hawkins, A. J. (2017, July 28). *How Tesla changed the auto industry forever*. (The Verge) Retrieved November 21, 2018, from theverge: https://www.theverge.com/2017/7/28/16059954/tesla-model-3--2017-auto-industry-influence-elon-musk

Hawkins, A. J. (2018, June 7). *Tesla's Autopilot steered car toward barrier before deadly crash, investigators say*. Retrieved from the verge : https://www.theverge.com/2018/6/7/17438194/tesla-autopilot-fatal-crash-ntsb-report

Hawley, G. (2017, August 06). *UNDERSTANDING TESLA'S LITHIUM ION BATTERIES*. Retrieved from Evan Nex: https://evannex.com/blogs/news/understanding-teslas-lithium-ion-batteries

Hess, R. A. (2014). A model for pilot control behavior in analyzing potential loss-of-control events . *Institution of MECHANICAL ENGINEERS*.

Hill, M. (2005). Control Systems . In M. Hill, *The Electronics Engineers' Handbook 5th Edition* (p. Section 19).

Hogenson, J. (n.d.). *PID for Dummies*. Retrieved from Csimn: https://www.csimn.com/CSI_pages/PIDforDummies.html

Honeywell, D. (2000). PID Control. In D. Honeywell.

HYE. (2018, February 11). *Everything you wanted to know about Tesla's electric car batteries*. Retrieved from Hibridosyelectricos:

Awab Syed
https://www.hibridosyelectricos.com/articulo/mercado/todo-querias-saber-baterias-coches-electricos-tesla/20180209151346017420.html

International Organization for Standardization. (1977). *ISO 3833:1977.* Retrieved from ISO: https://www.iso.org/standard/9389.html

jBEAM. (n.d.). *Engine Test Bench*. Retrieved from Amsoline: https://www.amsonline.de/en/applications/automobile-rd/engine-test-bench/

K. Astrom, T. H. (2005). Advanced PID Control . *Instrument Society of America*.

Kenny. (2015). *[Tech] Motor Inductance, Resistance and Maximum RPM: Estimated vs Actual*. Retrieved from Teslamotorsclub: https://teslamotorsclub.com/tmc/threads/tech-motor-inductance-resistance-and-maximum-rpm-estimated-vs-actual.46353/

Kirkland, G. (2017, 06 01). *How new technologies have changed the automotive industry*. Retrieved November 21, 2018, from oponeo: https://oponeo.co.uk/tyre-article/how-new-technologies-have-changed-the-automotive-industry

Knowles, D. D. (2016-17, September). *Final Year Project ENX313.* Retrieved November 21, 2018, from canvas: https://canvas.sunderland.ac.uk/courses/27195/pages/module-handbook?module_item_id=263998

Lambert, F. (2018, January 19). *Tesla introduces new Model S wheels with updated design*. Retrieved January 13, 2019, from Electrek: https://electrek.co/2018/01/19/tesla-new-model-s-wheels-updated-design/

Levin, S. (2018, April 13). *Tesla email reveals company's effort to silence an alleged victim with cash* . Retrieved from theguardian: https://www.theguardian.com/technology/2018/apr/12/tesla-media-strategy-discrimination-car-crash

Li, Y. &. (2006). *PID control system analysis and design. IEEE Control Systems Magazine* . University of Glasgow.

Lin, P. (2017, April 5). *Here's How Tesla Solves A Self-Driving Crash Dilemma* . Retrieved from Forbes : https://www.forbes.com/sites/patricklin/2017/04/05/heres-how-tesla-solves-a-self-driving-crash-dilemma/#71944bf76813

Liu, W. (2017). *Hybrid Electric Vehicle System Modeling and Control.*

Mckinsey & Company . (2014, March). *Are you ready for the resource revolution?* Retrieved from Mckinsey: https://www.mckinsey.com/business-functions/sustainability/our-insights/are-you-ready-for-the-resource-revolution

Mckinsey Center for Future Mobility. (2018, March). *What a teardown of the latest electric vehicles reveals about the future of mass-market EVs*. Retrieved from Mckinsey: https://www.mckinsey.com/industries/automotive-and-assembly/our-insights/what-a-teardown-of-the-latest-electric-vehicles-reveals-about-the-future-of-mass-market-evs

McMahon, J. (2018, Jun 27). *How Tesla Scored A Zero On Climate Management*. Retrieved from Forbes: https://www.forbes.com/sites/jeffmcmahon/2018/06/27/how-tesla-earned-a-zero-score-for-climate-management/#46046c012e2f

mcMahon, J. (2018, June 27). *How Tesla Scored A Zero On Climate Management* . Retrieved from Forbes : https://www.forbes.com/sites/jeffmcmahon/2018/06/27/how-tesla-earned-a-zero-score-for-climate-management/#2e93819c2e2f

Mishra, K. S. (2014). *Comparative Study of P, PI and PID controller for speed control of VSI-fed induction motor.* India: SSTC Bhilai.

Moss, D. (2018, October 18). *History of the electric car*. Retrieved November 18, 2018, from whatcar: https://www.whatcar.com/news/history-of-the-electric-car/n18063

Mpanda, K. A. (n.d.). *PID Control Theory*. ESIEE - Amiens, France, South Africa : University of Nancy, Teaching and Research at the University of Picardie.

Msstarlabs. (n.d.). *Introduction*. Retrieved from Msstarlabs: http://www.mstarlabs.com/control/znrule.html

Muir, A. (2019). *Wheels and Tyres*. Retrieved from Howacarworks: https://www.howacarworks.com/blog/making-it-easier-to-see-how-cars-work

National Instruments . (n.d.). *PID Theory Explained*. Retrieved from National Instruments : http://www.ni.com/en-gb/innovations/white-papers/06/pid-theory-explained.html

P567, C. (n.d.). *Lecture 9 - Implementing PID Controllers* .

Taherian, H. (2014). AERODYNAMICS OF INTERCITY BUS AND ITS IMPACT ON CO2 REDUCTIONS. *UAB School of Engineering - ECTC 2014 Proceedings - Vol. 13*.

Temel, S. (n.d.). *P, PD, PI, PID Controllers.* Middle East Technical University: Electrical and Electronics Engineering Department .

Tesla - Model S - P85 PERFORMANCE (416Hp). (n.d.). Retrieved from auto-data: https://www.auto-data.net/en/tesla-model-s-p85-performance-416hp-18612

Wakefield. (1993). *HISTORY OF THE ELECTRIC AUTOMOBILE BATTERY-ONLY POWERED CARS.* Warrendale, PA, United States : Society of Autmotive Engineers .

8. Appendices

8.1. Appendix A – Project Synopsis / Scope

Model Tesla S P85 and design speed control system

Project Scope Form	
Project Title: Model Electric Car based on Tesla Model & Design Speed Control System	**Student Number:** 118 616 4302
Project Leader/Manager: Awabullah M Syed	**Anticipated Project Start Date:** 5th Nov 2018
Supervisor: Kevin Burn	**Date Prepared:** 25th Oct 0218
University: Sunderland	**Estimated Completion Date:** 15th April 2019

Purpose of Project:

The project will begin with a review of existing literature, involving patent search, articles, and books and published academic work etc. (Knowles, 2016-17). A mathematical model representing the Tesla Model S P85 will be constructed to execute an in-depth analysis of the vehicle's dynamics to evaluate the battery performance, motor, wheels and other potential components that could influence the Simulink model. The mathematical model would then be translated to the MATLAB Simulink with the help of functional blocks, transfer functions and closed-loop model.

Control systems to be designed and implemented in the Simulink model to regulate the speed of the Tesla Model S P85. A range of control systems would be considered and compared with respect to their limitations. The control systems implemented would be tuned using some sort of algorithms to suit the set parameters.

It should be noted that driverless vehicle will not be considered nor analysed however, the potential impact the speed control system would have on it will be evaluated. Though, the results obtained from the Simulink Model is solely be based on Tesla Model S P85.

Awab Syed

Stakeholders:

Internal

- Awabullah Syed – Author
- Kevin Burn – Supervisor
- Derek Dixon – Project Leader

External

- University of Sunderland
- Tesla Inc
- Government legislations

Resource Requirements:

- MATLAB
- Primary data – knowledgebase & web documentation

Approvals:

Name, Signature, Date

Awab Syed, 25th December 2018

Requested by: Awabullah M. Syed

Name, Signature, Date

Kevin Burn, 25th December 2018

Approved by Kevin Burn

8.2. Summary of Meeting Records

Date	Discussion	Action
07-11-2018	Discussed project options • Model Tesla and Design Speed Control System Other alternatives	Define; research topics, start collecting papers, books
28-11-2018	• Building simple model	• Gain expertise in MATLAB • Aim to build DC motor
12-12-2018	• New project synopsis written • Created Simulink Model	• Full explanation of the model structure
15-01-2019	Literature Review in progress	• To complete literature review Consider potential controllers
06-03-2019	• Literature review completed • Simulink Model completed	• Consider controllers and tuning methods
14-03-2019	• Used autotune and manual tuning methods	Compare the result obtained
24-04-2019	Completed documenting the report	Revise

8.3. Appendix C – m-file / Model Parameters

```
KT = 0.25;
R = 5.3*10^-3;          % Actual Armature Resistance
L = 493*10^-9;          % Inductance
KE = 0.12;              % Back EMF
JM = 0.4;               % Moment of inertia of the rotor
b = 0.1;               % Damping Coefficient

```

Figure 58 - m-file displaying the physical parameters of Block Tesla Motor Model

```
Sc = 2*pi;              % Scaling Factor
Cw = 2*pi*0.24;         % Wheel Circumference
Rg = 9.73;              % Gear Ratio
KE = 0.12;              % Back EMF
Reference_Input = 50;
Scaling_Velocity = Sc/(Cw)*Rg*KE;

KT = 0.25;              % Torque Constant
L = 493*10^-9;          % Inductance
R = 5.3*10^-3;          % Actual Armature Resistance
Ts = 0.01;
```

Figure 59 - m-file displaying the physical parameters of the control system